Transverse systems along the extensional Tyrrhenian margin of central Italy and their influence on volcanism

Valerio Acocella[1] and Renato Funiciello[1]

Received 5 May 2005; revised 17 November 2005; accepted 16 December 2005; published 16 March 2006.

[1] The Tyrrhenian margin of central Italy has undergone Plio-Quaternary extension, developing NW-SE normal faults and NE-SW faults. The NE-SW faults decrease in frequency toward NE with the stretching factor β, becoming negligible for $\beta < 1.3$. Plio-Quaternary volcanoes, aligned NW-SE, formed at the intersection among NE-SW and NW-SE faults; fissure eruptions are mostly controlled by NE-SW faults. Structural field data show normal motions for 76% of NW-SE Quaternary faults and transtensive for 73% of NE-SW Quaternary faults. Analogue experiments simulating the NE-SW Tyrrhenian extension show that transverse transtensive faults form with differential extension $\Delta\beta > 0.21$. These data suggest that the NE-SW transtensive structures are transfer faults of the NW-SE normal faults due to relevant differential extension ($\Delta\beta > 0.21$) within a stretched crust ($\beta > 1.3$). The minor dip-slip and strike-slip components of the NE-SW and NW-SE faults, respectively, possibly result from the NW-SE extension due to the southeastward slab retreat beneath the Calabrian arc. The NE-SW and NW-SE extensions in the central southern Tyrrhenian Sea account for the composite kinematics of the NE-SW structures, which, in turn, exert a twofold role in controlling volcanism. Where their dip-slip component forms basins, the associated decompression induces magma accumulation (developing central volcanoes) at the intersection among NW-SE and NE-SW systems. Where transfer faults are mainly strike slip, their inferred subvertical attitude enhances their permeability to magma, accounting for the observed NE-SW fissure eruptions. Regional extension, forming NW-SE faults, enhances the overall generation and rise of magma along the margin, but NE-SW structures focus magma rise and emplacement at shallower levels. **Citation:** Acocella, V., and R. Funiciello (2006), Transverse systems along the extensional Tyrrhenian margin of central Italy and their influence on volcanism, *Tectonics*, *25*, TC2003, doi:10.1029/2005TC001845.

[1]Dipartimento Scienze Geologiche, Università Roma Tre, Rome, Italy.

0278-7407/06/2005TC001845

1. Introduction

[2] Rift zones are characterized by subparallel segments (with strike variations lower than few tens of degrees) of normal faults, perpendicular to the least compressive stress. This is commonly observed in various continental and oceanic settings, such as the East African Rift System [*Morley*, 1988; *Ebinger*, 1989a, 1989b; *Ebinger et al.*, 1989; *Morley et al.*, 1990; *Nelson et al.*, 1992], the Rio Grande Rift [*Cordell*, 1978; *Mack and Seager*, 1995], the Rhine Graben [*Illies*, 1975; *Brun et al.*, 1991], the Baikal Rift [*Sherman*, 1978; *Hutchinson et al.*, 1992], the Basin and Range [*Anders and Schlische*, 1994; *Ferrill et al.*, 1999], and the Icelandic Ridge [*Acocella et al.*, 2000].

[3] However, additional fault systems, with a remarkably different strike, may form simultaneously to the main set of normal faults. In many cases, these systems, when subparallel to the extension direction, have been interpreted as transfer faults of the normal faults, such as at the North Sea [*Gibbs*, 1984], the Atlantic margin of Brazil [*Milani and Davison*, 1988], of Newark [*Schlische*, 1992], Galicia [*Boillot et al.*, 1995], West Africa [*Clemson et al.*, 1997; *Watts and Stewart*, 1998], Norway [*Dorè et al.*, 1997; *Tsikalas et al.*, 2001], the Suez Rift [*McClay and Khalil*, 1998], the Basin and Range [*Martin et al.*, 1993; *Duebendorfer and Black*, 1992], and the East African Rift System [*Rosendahl*, 1987; *Faulds and Varga*, 1998]. In other cases, three-dimensional strain [*Reches*, 1978; *Krantz*, 1989] and viscosity or density instabilities [*Watterson et al.*, 2000] have been proposed to explain the development of transverse faults under a constant extensional regime. In several settings, such as along the Mexican Volcanic Belt [*Tibaldi*, 1992], the central Andes [*Riller et al.*, 2001; *Matteini et al.*, 2002], the Ethiopian Rift [*Acocella et al.*, 2002], the Western Branch of the East African Rift System [*Ebinger*, 1989a; *Ebinger et al.*, 1989], and the Rio Grande Rift [*Cordell*, 1978], the transverse systems also control the location of volcanic activity and the shape of volcanoes. This suggests that transverse systems may significantly control the evolution of rift zones and associated magmatism. Previous studies investigated the relationships between transverse systems and magmatism. Analogue models highlighted the role of extensional tectonics, responsible for developing transfer faults and controlling the localized rise of melts [*Acocella et al.*, 1999; *Corti et al.*, 2002, 2004]. Other studies suggested that conversely, the emplacement of magma at depth may influence the development of transverse zones at surface [*Ruppel*, 1995; *Faulds and Varga*, 1998].

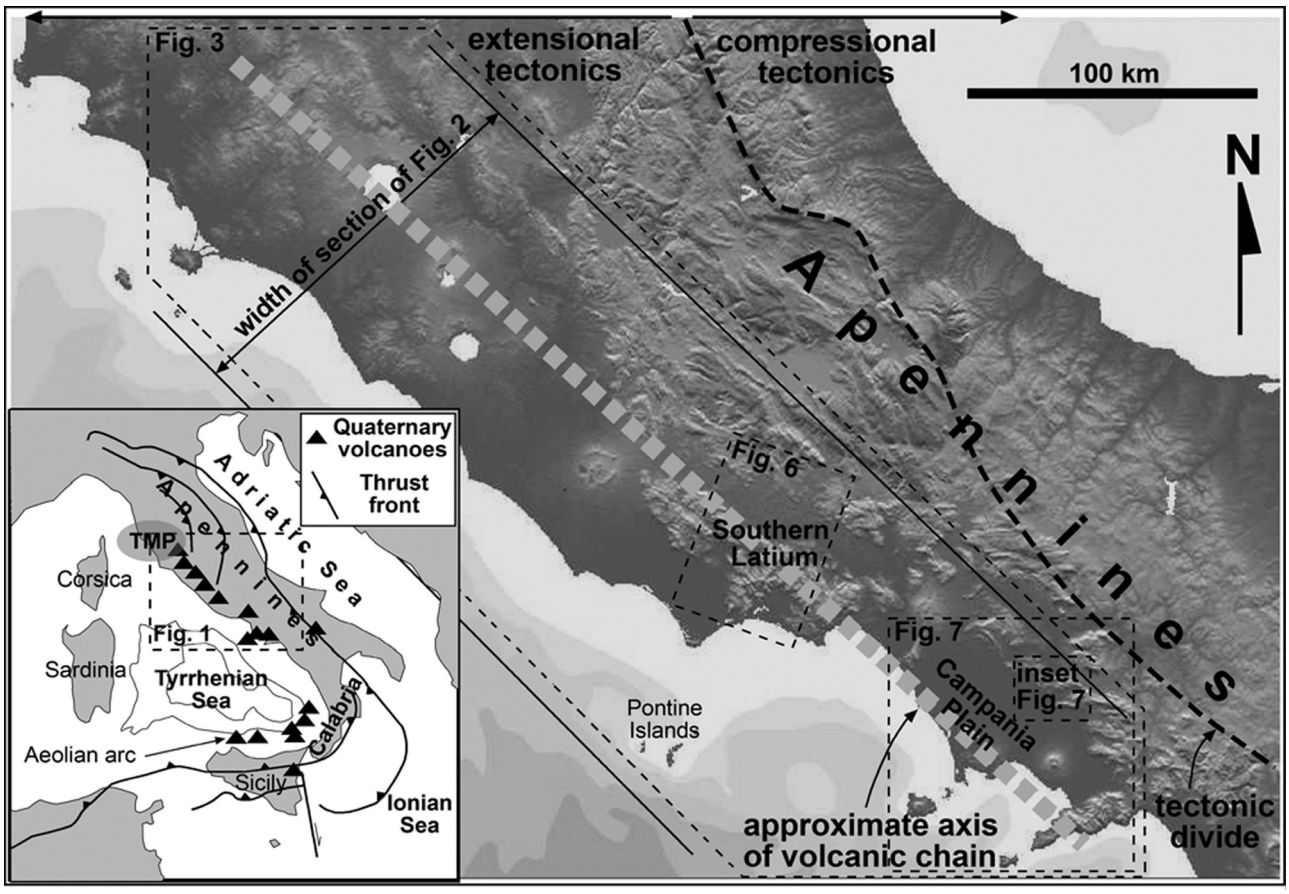

Figure 1. Digital elevation model of the central Apennines, showing the present tectonic divide (heavy black dashed line) between the eastern portion, undergoing compression, and the western portion, undergoing extension. Inset shows a structural sketch of the Italian peninsula, characterized by arcuate thrust fronts (distinguished on the base of their age) and, to the back, in the Tyrrhenian area, extension and volcanism. TMP, Tuscan Magmatic Province. Figures 6 and 7 refer to the areas of southern Latium and Campania Plain, respectively.

[4] The Tyrrhenian margin of central Italy has been characterized by Plio-Quaternary back-arc extension, with the development of NW-SE normal faults; coeval NE-SW transverse systems are also present and the margin exhibits orthogonal fault sets simultaneously developed under an extensional setting. Moreover, the NE-SW structures are predominant at volcanic edifices and control eruptive fissures, showing an important influence on Plio-Quaternary back-arc volcanism, despite its overall NW-SE alignment [*Acocella and Funiciello*, 2002]. Therefore among the most interesting features of the Tyrrhenian margin are the development of orthogonal structures under extension and their control on volcanic activity.

[5] Within this framework, this paper aims at defining (1) the structural features (geometry and kinematics) of the orthogonal systems characterizing the extension of the Tyrrhenian margin, as well as their relationships and (2) their possible control on the Plio-Quaternary magmatism. With these aims, field structural data have been collected at selected locations (outside the volcanic areas) along the margin; these have been integrated with results from previously performed analogue experiments simulating the Tyrrhenian extension, as well as with an original overview of the structure of the volcanic areas. The results suggest that different structures control magmatism at different crustal levels along the Tyrrhenian margin, similarly to other areas worldwide (Tuscan Magmatic Province, in Italy, Ethiopian Rift, central Andes, Mexican Volcanic Belt, Western Branch of the African Rift System).

2. Structural Setting of the Tyrrhenian Margin of Central Italy

[6] Extensional processes have been affecting the Tyrrhenian margin of the Italian peninsula since the upper Miocene [*Jolivet et al.*, 1998, and references therein]. Extension occurred at the back of the eastward migrating Apennine orogen, as a consequence of the progressive eastward shifting of the Apennine subduction, largely driven by the subducting oceanic lithosphere beneath the Calabrian arc (Figure 1 inset) [*Malinverno and Ryan*, 1986; *Royden et al.*, 1987; *Patacca et al.*, 1990; *Jolivet et al.*,

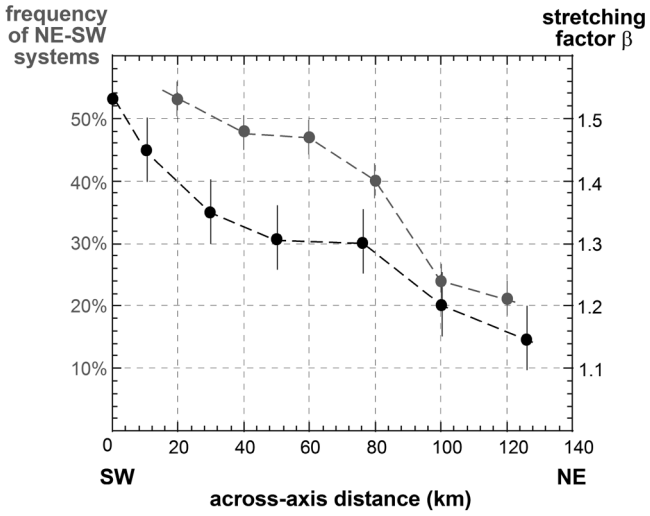

Figure 2. Variation of the stretching factor β (grey) and frequency of the NE-SW systems across the Tyrrhenian margin (normalized to the NW-SE normal faults in the area between the two parallel solid lines in Figure 1; these faults are shown in Figure 3).

1998]. Along the Tyrrhenian margin of central Italy, active extensional tectonics migrated eastward, from the Tyrrhenian area (mostly during the Miocene-Pliocene) to the Apennines divide (Present), where the boundary between the extensional and compressional domains is approximately located (Figure 1) [*D'Agostino et al.*, 1998; *Ghisetti and Vezzani*, 2002]. While the eastern part of the divide is characterized by active compression, the western part is presently marked by extension and associated with seismic activity due to NW-SE normal faulting [*Montone et al.*, 1999; *Valensise and Pantosti*, 2001, and references therein; *D'Agostino et al.*, 2001; *Roberts and Michetti*, 2004]. The development of these NW-SE normal faults is interpreted as resulting from the retreat of the westward dipping slab, highlighted by tomography data [*Spakman and Wortel*, 2005], beneath the central northern Apennines, in an overall context of back-arc extension [*Faccenna et al.*, 1997; *Jolivet et al.*, 1998]. The NW-SE normal faults responsible for the extension of the area between the Tyrrhenian Sea and the Apennines divide are also responsible for the development of several subparallel Plio-Quaternary basins (Figure 1) [*Mariani and Prato*, 1988; *Cavinato et al.*, 1994]. Many of the NW-SE normal faults reactivate preexisting thrust planes, mostly SW dipping, formed during the buildup of the Apennines [*Faccenna et al.*, 1995; *D'Agostino et al.*, 1998]. Balanced cross sections from published works [e.g., *Spadini and Podladchikov*, 1996; *Faccenna et al.*, 1997; *Mele and Sandvol*, 2003] permit estimation of the stretching factor β across the Tyrrhenian margin. Assuming an overall symmetric extension across the Tyrrhenian basin [*Jolivet et al.*, 1998], the stretching factor in these balanced sections is evaluated as $\beta = t_i/t_f$ (where t_i is the initial thickness of the crust and t_f is the thickness of the stretched crust), that is, the thickness difference between a stretched portion of the margin and the portion in correspondence with the tectonic divide, which represents the preextension crustal thickness (Figure 1). This procedure, which neglects any possible Moho destabilization process [*Ziegler and Cloething*, 2004], shows that the NW-SE faults are responsible for a crustal stretching β increasing from the divide (where $\beta = 1$) to the Tyrrhenian coastline (where $\beta \sim 1.5$) (Figure 2). Along the margin, crustal stretching is not constantly distributed, for several reasons. On a general scale, extension migrates eastward and is driven by the arcuate configuration of the compressive front, whose shape is, in turn, controlled by the different nature of the subducted lithosphere: this is continental in the northern and central Apennines, oceanic in the southern Apennines [*Malinverno and Ryan*, 1986; *Royden et al.*, 1987]. As a result, the southern Tyrrhenian area (Figure 1) is characterized by larger amounts of extension with regard to the northern Tyrrhenian area [*Royden et al.*, 1987; *Patacca et al.*, 1990; *Doglioni et al.*, 2004]. This process has its repercussions, at a more local scale, also along the Tyrrhenian margin of central Italy. In fact, the subducting front during Miocene was located to the east of Sardinia and Corsica, with an overall N-S trend (Figure 1) [*Faccenna et al.*, 2001, and references therein]. Considering the present NW-SE orientation of the Tyrrhenian margin of central Italy, subparallel to the present subducting front to the east of the central Apennines, it appears that its southern part underwent a much larger amount of back-arc extension, resulting from the larger slab retreat in the southern Tyrrhenian area. Along the Tyrrhenian margin of central Italy, the variable amount of stretching is highlighted by (1) the structural and topographic variations in the lateral continuity of the extensional basins and (2) the different width of the extended area between the axis of the volcanic chain and the divide (Figure 1); this implies a different distribution of the amount of extension across the margin.

[7] NE-SW fractures often interrupt the continuity of adjacent NW-SE extensional basins on the margin (Figure 3) [*Acocella and Funiciello*, 2002]. In general, surface and subsurface data show that the NE-SW and the NW-SE systems crosscut each other at high angles (Figure 3) [*Acocella and Funiciello*, 2002, and references therein]. In many cases, NE-SW systems form transverse extensional basins [*Mariani and Prato*, 1988]. Seismic profiles suggest that these basins are bordered by several subparallel faults with a normal component, which join and become shallower at depths ~2–3 s (two-way traveltime, TWT); the basins are filled by Plio-Quaternary sedimentary and volcanic deposits, which in some cases, form rollover-like structures dipping toward the border faults [*Mariani and Prato*, 1988; *Faccenna et al.*, 1994a]. The frequency (normalized to the NW-SE normal faults) of the transverse structures, widespread along the margin, decreases significantly northeastward (Figure 2). In fact, immediately NE of the volcanic chain, few significant NE-SW structures are observed; these mostly formed as tear faults or lateral ramps during the compressional phase, possibly related to block rotations around vertical axes [*Mattei et al.*, 1995], and have

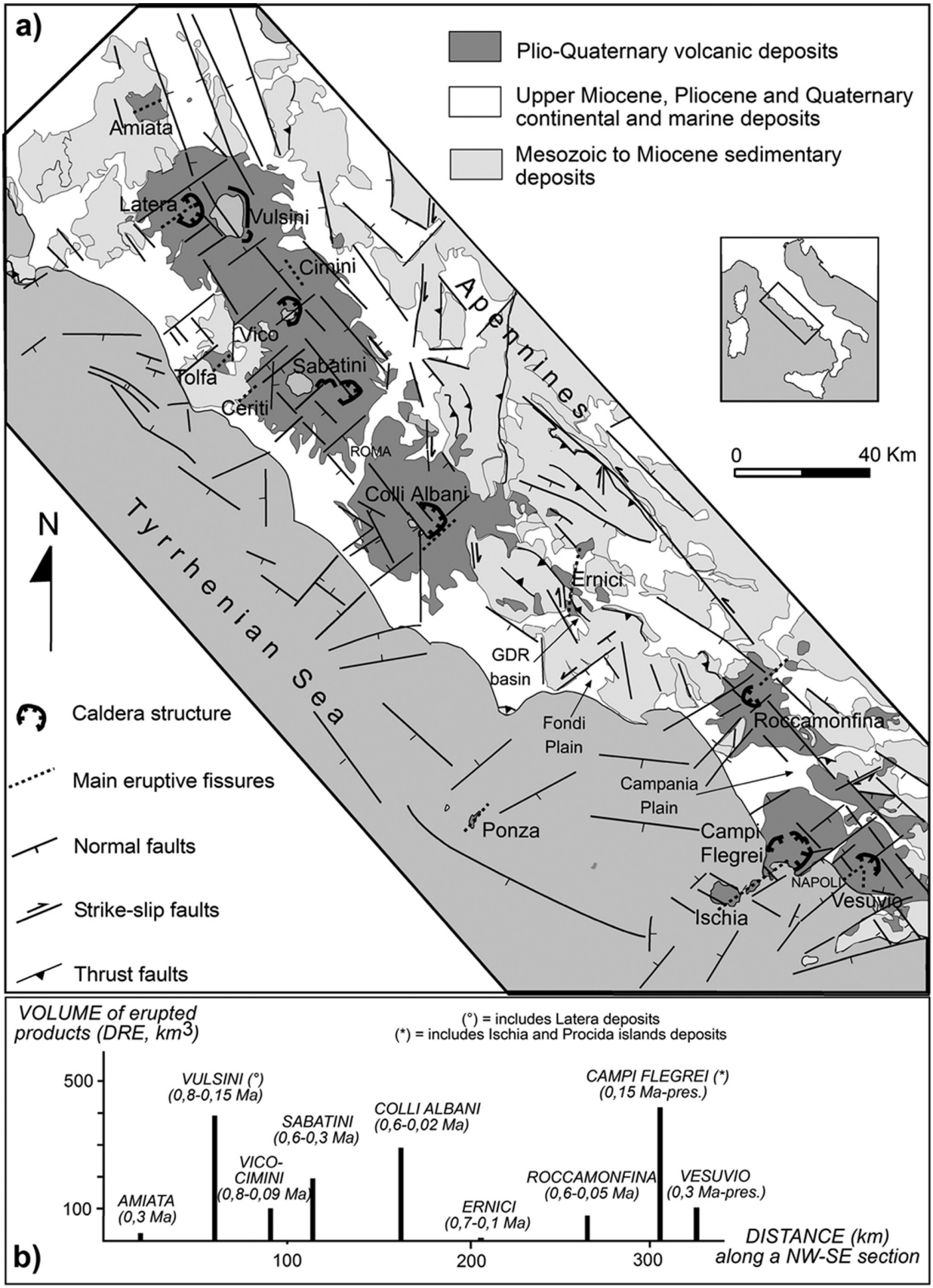
a)
Plio-Quaternary volcanic deposits
Upper Miocene, Pliocene and Quaternary continental and marine deposits
Mesozoic to Miocene sedimentary deposits
Amiata
Latera
Vulsini
Cimini
Vico
Tolfa
Sabatini
Ceriti
ROMA
Colli Albani
Ernici
Apennines
Tyrrhenian Sea
GDR basin
Fondi Plain
Campania Plain
Ponza
Roccamonfina
Campi Flegrei
NAPOLI
Vesuvio
Ischia
0
40 Km
N
Caldera structure
Main eruptive fissures
Normal faults
Strike-slip faults
Thrust faults
VOLUME of erupted products (DRE, km3)
(°) = includes Latera deposits
(*) = includes Ischia and Procida islands deposits
500
100
VULSINI (°) (0,8-0,15 Ma)
SABATINI (0,6-0,3 Ma)
COLLI ALBANI (0,6-0,02 Ma)
CAMPI FLEGREI (*) (0,15 Ma-pres.)
VICO-CIMINI (0,8-0,09 Ma)
ROCCAMONFINA (0,6-0,05 Ma)
VESUVIO (0,3 Ma-pres.)
AMIATA (0,3 Ma)
ERNICI (0,7-0,1 Ma)
b)
100
200
300
DISTANCE (km) along a NW-SE section

Figure 3

been moderately reactivated as strike-slip faults during extension (Figure 3) [*Ghisetti and Vezzani*, 1997, 1999].

[8] The coeval activity of NW-SE and NE-SW fractures, as well as their joint eastward migration, has been recognized in sedimentary and volcano-tectonic depressions along the Tyrrhenian margin [*Acocella and Funiciello*, 2002, and references therein]. While the NW-SE systems are responsible for crustal extension along the margin, the role of the NE-SW systems is more debated. Transverse structures along the Apennines may result from the reactivation of lateral ramps developed during the previous compressional phase [*Ghisetti and Vezzani*, 1997, 1999]. Transverse structures have also been interpreted as the result of longitudinal extension due to the curvature of the Apennines [*Oldow et al.*, 1993]. This mechanism may easily account for orogen-parallel extension along the southern Apennines, where the orogen curvature is significant; however, it may not be easily applied to the central Apennines, where the curvature of the arc is much lower and the transverse structures are mostly restricted to the back-arc domain. Alternatively, NE-SW fractures, being coeval to NW-SE systems, have been interpreted as transfer systems of the NW-SE normal faults [*Liotta*, 1991; *Faccenna et al.*, 1994a; *Acocella et al.*, 1999], but this hypothesis is not confirmed by robust data. A further possibility is that the NE-SW faults are the effect of the NW-SE extension in the southern Tyrrhenian area, resulting from the Quaternary SE retreat [*Patacca et al.*, 1990] of the oceanic Ionian slab subducting beneath the Calabrian arc. This hypothesis is consistent with the Quaternary age of most of the transverse basins along the margin [*Mariani and Prato*, 1988], even though some formed during the Pliocene [*Faccenna et al.*, 1994a]. The lack of published geometric and kinematic data on transverse structures does not currently permit to discriminate among these hypotheses.

[9] In addition to NE-SW and NW-SE systems, the Quaternary evolution of the Tyrrhenian margin has been partly accompanied by N-S trending structures. These are much less represented and of more limited extent, even though are scattered throughout the margin [*Funiciello et al.*, 1976; *Alfonsi et al.*, 1991; *Faccenna et al.*, 1994b, and references therein; *Acocella et al.*, 1996; *Marra*, 2001; *Sani et al.*, 2004].

3. Plio-Quaternary Volcanoes and Their Structural Features

[10] Potassic volcanism accompanied extension [*Serri et al.*, 1993]. The Plio-Quaternary volcanoes are NW-SE aligned, parallel to the regional normal faults. The volcanic arc consists of (1) central edifices, characterized by calderas with negligible topographic relief (Vulsini, Sabatini, Campi Flegrei) and stratovolcanoes with summit calderas (Vico, Colli Albani, Roccamonfina and Vesuvio), and (2) major fissure eruptions (extent larger than a few kilometers: Amiata, Vulsini, Cimini, Colli Albani, Roccamonfina, Campi Flegrei and Vesuvio; Figure 3a). Fissure eruptions refer to the alignment of vents, with common composition, not necessarily active contemporaneously, although active within a limited time span compared to the life of the related volcano. Several of these major eruptive fissures are related to the activity of the nearby central edifices. The mean spacing of the volcanoes is 42±13 km; the low standard deviation (13 km) implies a quite regular distribution. However, this does not correspond to an uniform distribution of the erupted volumes, with most magma being usually (Colli Albani is the exception) erupted at Quaternary calderas with negligible relief (Vulsini, Sabatini, and Campi Flegrei; Figure 3b).

[11] On the basis of the distinction between central edifices and fissure eruptions, an overview of the structural features of the volcanoes, resulting from published surface and subsurface data, is proposed.

3.1. Main Volcanic Edifices

[12] Vulsini District (0.80–0.15 Ma) erupted undersaturated leucite bearing magmas and differentiates [*Nappi et al.*, 1987]. The main feature is the down-sag Bolsena Caldera (Figure 4a), along a NW-SE trending graben (Figure 3a). A NE-SW graben-like structure partly controls volcanic activity within the NE-SW elongated Latera Caldera (0.60–0.10 Ma) (Figure 4a) [*Vezzoli et al.*, 1987; *Nappi et al.*, 1991]. Vico District (0.80–0.09 Ma) erupted alkaline potassic lavas, forming a caldera at the intersection between NW-SE and NE-SW faults (Figure 3a) [*Locardi et al.*, 1976; *La Torre et al.*, 1981]. Sabatini District (0.60–0.08 Ma) mainly erupted trachytic-phonolitic products, forming the down-sag Bracciano caldera (along a NE-SW graben) and the Sacrofano Caldera (Figure 4b) [*De Rita et al.*, 1993]. The district lies at the intersection among swarms of NW-SE and NE-SW structures [*Funiciello et al.*, 1976; *Locardi et al.*, 1976; *De Rita et al.*, 1996]. Colli Albani District (0.60–0.02 Ma) mainly erupted leucititic magmas at the intersection among swarms of NW-SE normal faults, NE-SW structures and N-S dextral faults (Figure 4c) [*De Rita et al.*, 1995]. A NE-SW Plio-Quaternary basin lies to the SW; the NE continuation of its border faults marks the caldera rim, feeding NE-SW aligned vents [*Faccenna et al.*, 1994a]. Roccamonfina District (0.60–0.05 Ma) erupted strongly undersaturated leucite-bearing rocks and LK magmas, forming a summit caldera at the intersection between NW-SE and NE-SW Plio-Quaternary grabens associated with hydrothermal circulation (Figure 4d) [*Mariani and Prato*, 1988; *Giordano et al.*, 1995; *De Rita and Giordano*, 1996; *Bosi and Giordano*, 1997]. The NE-SW elongated Campi Flegrei District includes the Campi Flegrei Caldera

Figure 3. (a) Structural sketch of the Tyrrhenian margin of central Italy, showing the main fault systems and the Plio-Quaternary volcanoes. (b) Spacing of volcanoes and related erupted volumes (estimates from *Barberi et al.* [1994], *De Rita et al.* [1992], *Orsi et al.* [1996], *Santacroce* [1987], *van Bergen and Barton* [1984], and *Bruno et al.* [2004]) along a NW-SE section.

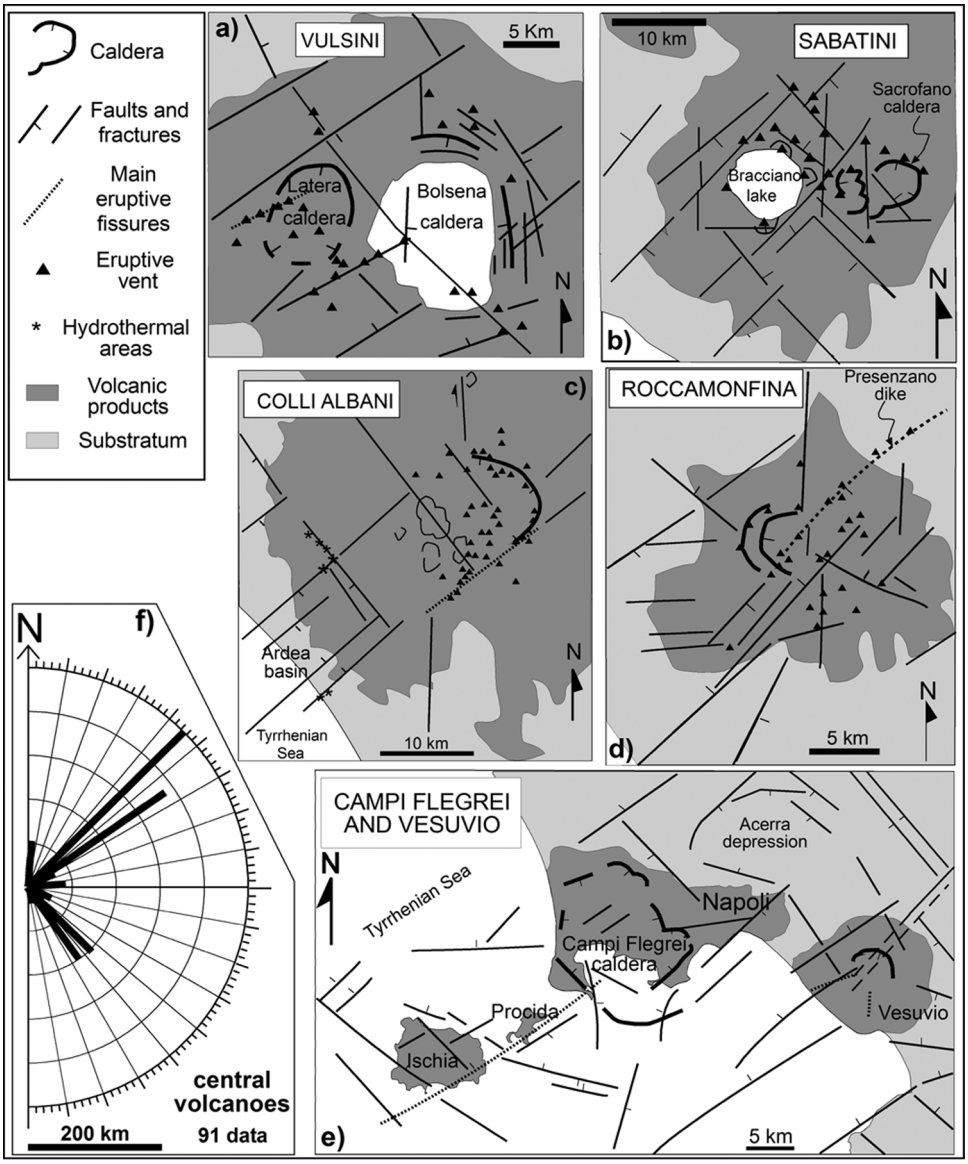

Figure 4. Structural sketch of the main volcanic edifices along the margin: (a) Vulsini District; (b) Sabatini District; (c) Colli Albani District; (d) Roccamonfina District; (e) Neapolitan volcanic area; and (f) strike distribution of all the fault systems located in the areas of the volcanic edifices.

and Ischia and Procida islands (Figure 4e) [*Carrara et al.*, 1973; *Finetti and Morelli*, 1974; *Fedi and Rapolla*, 1987; *Rapolla et al.*, 1989; *Orsi et al.*, 1996; *Piochi et al.*, 2005, and references therein]. The erupted magmas (0.15 Ma to Present) range from trachytes and alkali trachytes to trachybasalts, and latites [*Rosi and Sbrana*, 1987]. NE-SW and subordinate NW-SE extensional structures predominate, controlling the shape of the Caldera and resurgence at Ischia [*Orsi et al.*, 1996; *Acocella and Funiciello*, 1999]. NE-SW systems border the Plio-Quaternary Acerra Depression, ~3 km deep, to the west of the Caldera [*Scandone et al.*, 1991; *Berrino et al.*, 1998]. Somma-Vesuvio District (0.3 Ma to Present) mainly erupted phonolites and trachybasalts at the intersection among NW-SE, NE-SW, and, subordinately, N-S structures (Figure 4e) [*Santacroce*, 1987; *Piochi et al.*, 2005, and references therein]. These control the emplacement of the fissures on the volcano slopes. Gravity and seismic data show that Vesuvio lies along a major NE-SW structure, offsetting NW-SE normal faults [*Berrino et al.*, 1998; *Bruno et al.*, 1998].

[13] The strike distribution of the fracture systems in the central volcanic edifices (Figure 4f) shows that the longest systems trend NE-SW (N40°E–N60°E); NW-SE structures (N30°W–N50°W) constitute 46% of the NE-SW systems. The volcanic edifices show therefore a common structural control, mainly at the intersection between swarms of NE-

SW and subordinate NW-SE fractures; minor N-S systems are seldom present (Figure 4f). Edifices with lower amount of emitted products are usually associated with a single NE-SW trending set (Vico, Vesuvio; Figure 3). Edifices with higher amount of emitted products are usually associated with multiple transverse fractures, controlling the shape of calderas and bordering transverse basins (Vulsini, Sabatini, Colli Albani, Campi Flegrei; Figure 3). The transverse basins lie to the SW of the volcanoes (Vulsini, Sabatini, Colli Albani, Roccamonfina), except Acerra, to the NE. The known depth of the transverse basins is 1.3–3 km [*Mariani and Prato*, 1988; *Berrino et al.*, 1998] and the onset of sedimentation is 2–3 Ma older than the onset of the nearby volcanic activity [*Mariani and Prato*, 1988; *Faccenna et al.*, 1994a].

3.2. Main Fissure Eruptions

[14] Amiata volcanic edifice mainly results from a NE-SW fissure, erupting, at various points, rhyodacitic and minor mafic latitic lavas between 0.29 and 0.18 Ma [*Calamai et al.*, 1970; *Ferrari et al.*, 1996]. The NE-SW structural control, possibly related to strike-slip faults [*Fazzini and Gelmini*, 1982], is highlighted by the NE-SW trending gravity anomalies (Figure 5a) [*Orlando et al.*, 1991] and elongation of the K seismic horizon isobaths [*Gianelli et al.*, 1997]. At Vulsini, several vents at Latera form a NE-SW trending eruptive fissure, subparallel to the elongated Vepe Caldera (Figure 5b) [*Capaccioni et al.*, 1987; *Vezzoli et al.*, 1987; *Nappi et al.*, 1991]. The related products are the most primitive within the Vulsini District [*Peccerillo et al.*, 1987]. The earthquakes within the Latera Caldera are related to NE-SW subvertical sinistral faults [*Buonasorte et al.*, 1987]. Cimini District (Figure 3) is characterized by rhyolites to olivine-latites, mostly emplaced as lava domes aligned NW-SE [*Baldi et al.*, 1974; *Barberi et al.*, 1994]. Tolfa-Ceriti District consists of upper Pliocene silicic products, erupted from two fissures along NE-SW trending normal faults and, subordinately, N-S structures (Figure 5c) [*De Rita et al.*, 1994a, 1994b). The SE rim of the Colli Albani Caldera belongs to a 15 km long, NE-SW fissure (Figure 3) [*De Rita et al.*, 1995]. Ernici District consists of alkali basalts, latites, trachytes, and leucitites pyroclastic and lava vents (0.7–0.1 Ma [*Civetta et al.*, 1981, and references therein]), located along NW-SE, NE-SW, and N-S fractures [*Angelucci et al.*, 1974; *Acocella et al.*, 1996]. The longest fissure (~20 km, Latina Valley Fissure), N-S trending, is associated with dextral faults (Figure 5d) [*Acocella et al.*, 1996; *Sani et al.*, 2004] and erupted the lowest $^{87}Sr/^{86}Sr$ ratios of the NW Campania-Latium region [*Civetta et al.*, 1981; *Beccaluva et al.*, 1984; *Turi et al.*, 1991]. Ponza island (Figure 3) mainly consists of lower Pleistocene submarine silica-rich hyaloclastites and rhyolitic dikes, emplaced along a NE-SW direction, consistently with the recognized fracture pattern [*Carmassi et al.*, 1983; *De Rita et al.*, 2001]. Roccamonfina District has a major eruptive fissure (Figure 3), fed by a ~600 ka old NE-SW dike (Presenzano dike, Figure 4d), with the most primitive magmas in the district [*Acocella and Funiciello*, 2002]. At Campi Flegrei, several vents and dikes form a composite NE-SW fissure ~15 km long, associated with primitive magmas, from Ischia to Campi Flegrei Caldera (Figure 3) [*Di Girolamo and Rolandi*, 1975; *Beccaluva et al.*, 1984; *Poli et al.*, 1987; *Vezzoli*, 1988; *Civetta et al.*, 1991; *Acocella et al.*, 1999; *D'Antonio et al.*, 1999]. Somma-Vesuvio has two main historical flank fissures, trending NE-SW and N-S (Figure 4e) [*Santacroce*, 1987; *Marzocchi et al.*, 1993]. The longest NE-SW fissure erupted the most primitive products in the district [*Santacroce*, 1987].

[15] The major eruptive fissures on the margin are NE-SW trending (Figure 5e), showing a common structural control; the NE-SW fissures at Latera, Ernici, Campi Flegrei, and Vesuvio also erupted the most primitive products.

4. Definition of the NE-SW and NW-SE Fault Systems

4.1. Investigated Areas

[16] Structural field analysis was carried out to define the geometric and kinematic features of the NW-SE and the NE-SW structures along the margin. For this purpose, two sites have been selected in correspondence with major NE-SW and NW-SE lineaments: the southern Latium area and the NE portion of the Campania Plain (Figure 1). In particular, the area of southern Latium consists of a transect across the margin, along which measurements were made in correspondence of three areas: the Fondi Plain, The Giuliano di Roma (GDR) Basin, the Alatri area (Figure 6). These sites have been chosen because (1) they display evidence of major Quaternary tectonic activity, coeval to most volcanoes, related to both orthogonal systems; (2) they are distant from the main volcanic edifices, their geometry and kinematics should not be influenced by magmatic activity; and (3) the transect in southern Latium permits appreciation of any variation in the structural style across the margin.

4.1.1. Southern Latium Area

[17] This area is characterized by two main Quaternary depressions, the Fondi Plain and the GDR Basin, as well as by the Alatri area, where the deformations are of Pliocene-Quaternary age. The Fondi Plain consists of a ~20 × 10 km rhomboidal depression, elongated NE-SW (Figure 6). The depression is surrounded by Mesozoic limestones and filled by Quaternary deposits; these mainly consist of lower and middle Pleistocene marine and continental deposits [*Antonioli et al.*, 1990]. Gravity data suggest a depth of ~1 km for the central part of the depression [*Di Filippo and Toro*, 1980]. Its most striking structural feature is the NW border, marked by a ~20 km long NE-SW trending fault scarp, juxtaposing the Mesozoic limestones with the Quaternary deposits, largely responsible for the development of the nearby plain. This fault zone is one of the best exposed NE-SW trending structures along the margin and, to the SW, it probably continues to the Pontine Islands (Figures 1 and 3). It interrupts the continuity of the NW-SE normal fault

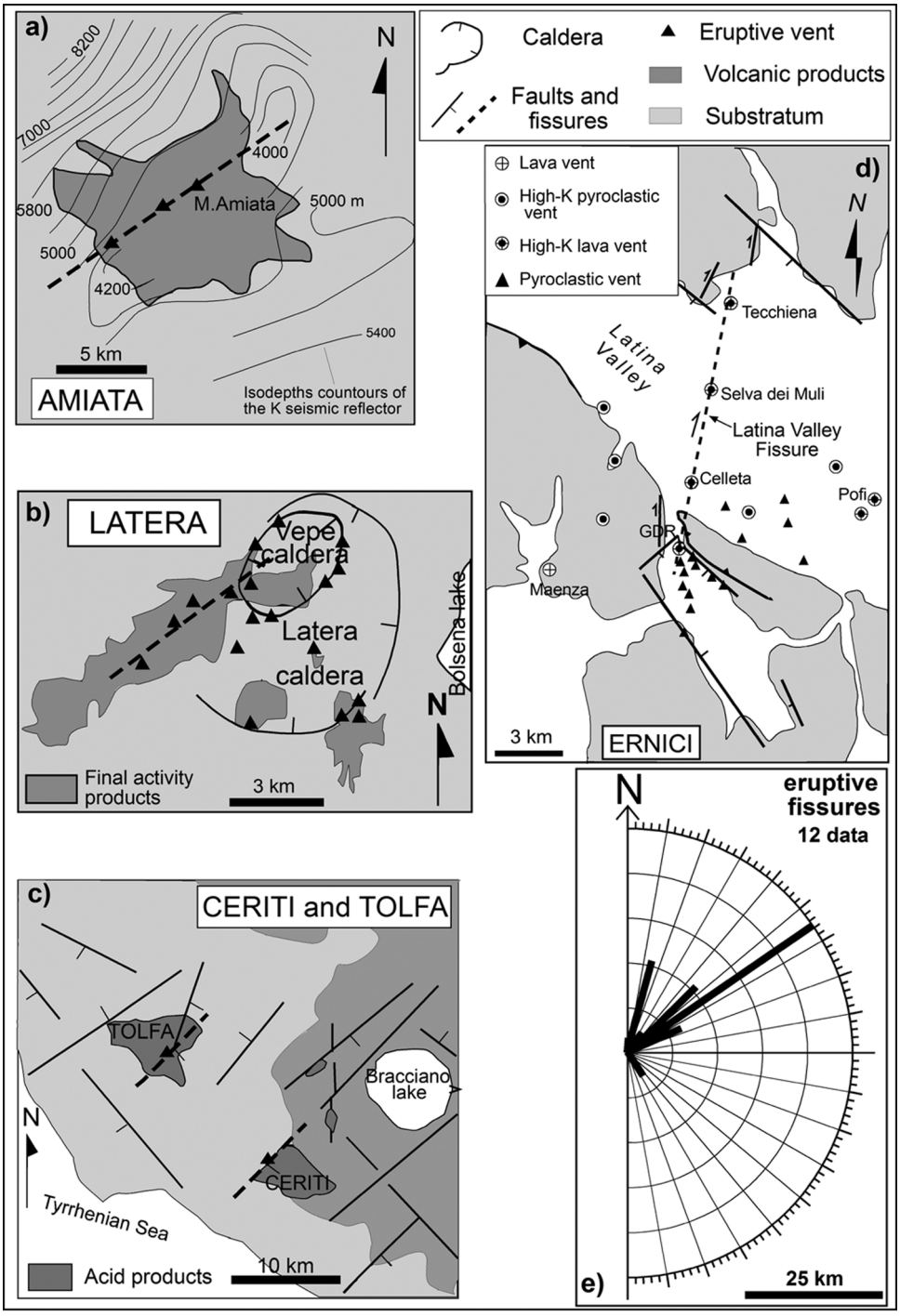

Figure 5. Structural sketch of the main fissure eruptions along the margin: (a) Amiata; (b) Latera; (c) Ceriti and Tolfa, (d) Ernici; and (e) strike distribution of the main fissure eruptions along the margin.

system that borders the NE part of the Fondi Plain (Figure 6); its morphology (Figure 6) suggests Quaternary activity, as confirmed by the different elevation of the middle Pleistocene deposits at the sides of the fault [*Antonioli et al.*, 1990]. No volcanism occurred within the Fondi Plain, which is therefore the most notable nonvolcanic transverse basin along the margin (Figure 3).

[18] Field work in the Fondi Plain was mainly focused along the NE-SW trending fault zone. The faults were mostly measured within Mesozoic limestones. Nevertheless, their association with major scarps with a young morphological expression, along which subsurface data indicate post-middle Pleistocene faulting [*Antonioli et al.*, 1990], suggests a Quaternary activity. The collected structural data

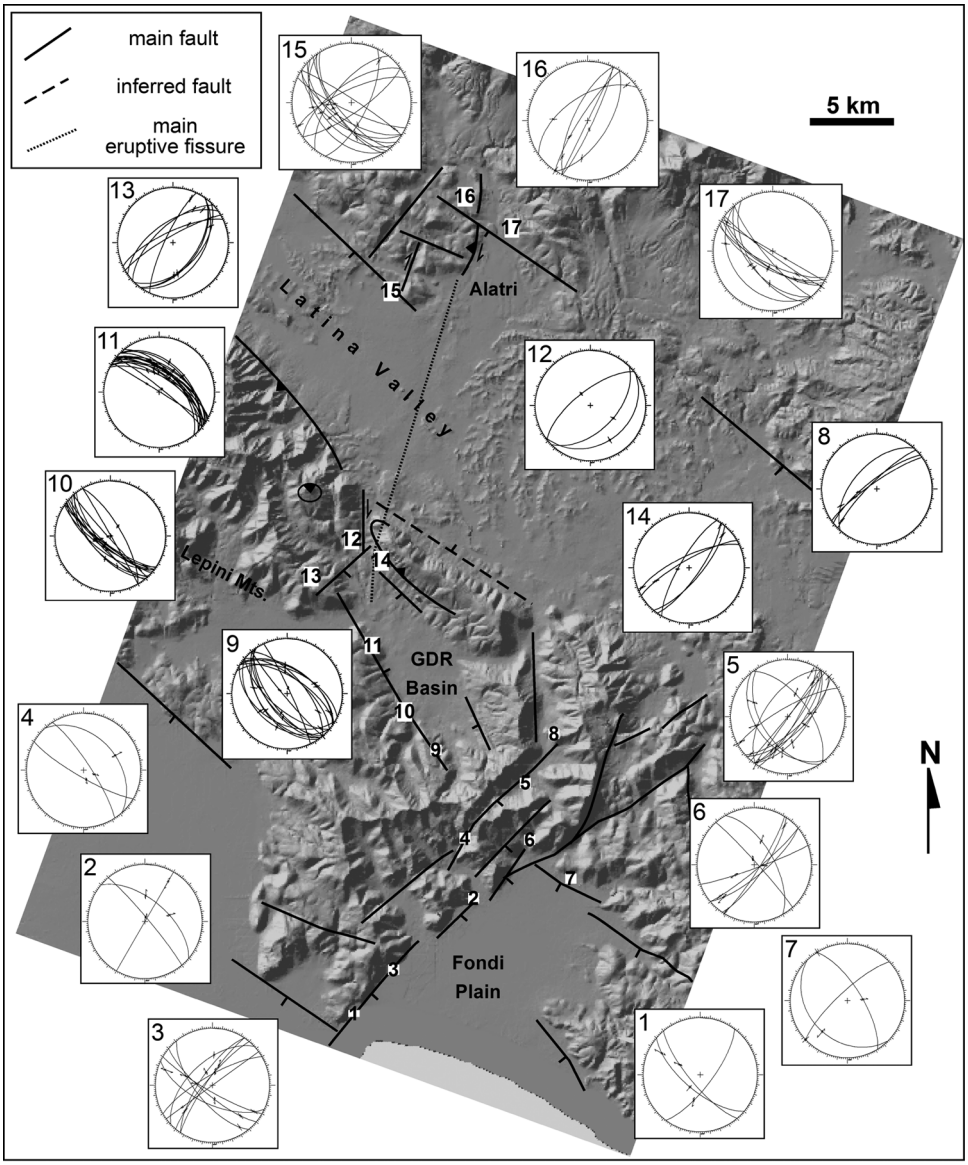

Figure 6. Simplified structural map of the southern Latium area (location in Figure 1), showing the major structures at the Fondi Plain, the GDR Basin, and the Alatri area. Sites of structural analysis and related plot (Schmidt's lower hemisphere) are also shown.

and their locations are displayed in Figure 6. The data consist of NW-SE and NE-SW faults systems which, despite the morphological evidence of the NE-SW faults interrupting the NW-SE faults (Figure 6), are repeatedly crosscutting each other. These fault systems are often associated with tectonic breccias and their mean displacement is of several tens of m.

[19] The GDR Basin is a NW-SE elongated Quaternary intramontane basin. The basin is bordered by Cretaceous limestones and filled with lower to middle Pleistocene lacustrine deposits and middle Pleistocene volcanics, produced by scattered vents of the Ernici District (Figure 6) [*Acocella et al.*, 1996]. The basin consists of a half-graben structure, with a maximum downthrow of ~800–1000 m. Its SW side is characterized by a major NW-SE normal fault, approximately 15 km long, partly controlling volcanic activity (Figure 6) [*Acocella et al.*, 1996]. The northern portion of this structure is partly interrupted by a ~2 km long NE-SW fault zone. The NE side of the basin is characterized by a ~4 km long NW-SE normal fault, controlling volcanic activity (Figure 6) [*Acocella et al.*, 1996]. Quaternary N-S dextral structures are also present, controlling part of the volcanic activity in the GDR Basin and the nearby Latina Valley (see section 3.2) [*Acocella et al.*, 1996; *Sani et al.*, 2004].

[20] Field work in the GDR Basin was focused along its SW border fault and the NE-SW structure in the northern part (Figure 6). The faults were mostly measured within Cretaceous limestones. Nevertheless, their associa-

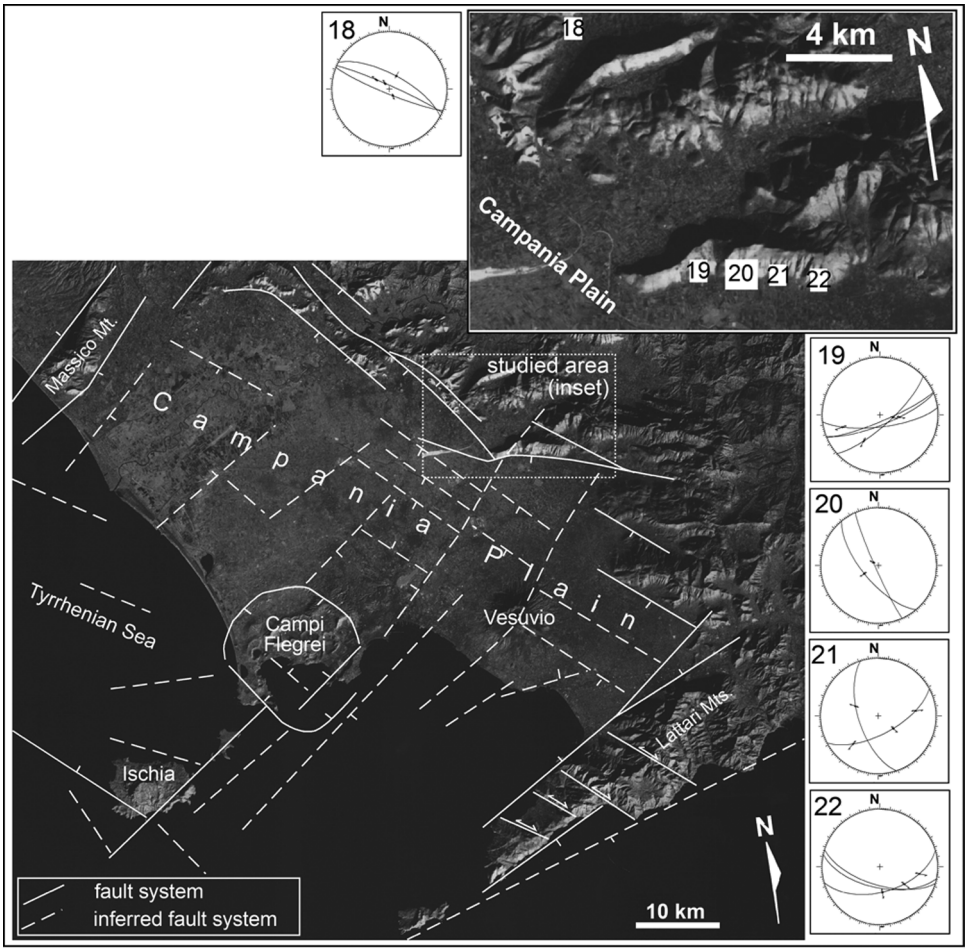

Figure 7. Satellite image of the Campania Plain (location in Figure 1) and its main fault systems (data are modified after *Acocella et al.* [2004, and references therein] and *Bruno et al. [2004*, and references therein]). Inset in the NE portion of the plain shows the area of structural analysis. Sites of structural analysis and related plot (Schmidt's lower hemisphere) are also shown.

tion with major scarps with a young morphological expression, developing a basin filled by Quaternary deposits, suggests a Quaternary activity. The collected structural data and their locations are displayed in Figure 6. The data consist of NW-SE and NE-SW faults associated with tectonic breccias, with a mean displacement of several tens of m.

[21] The Alatri area lies on the NE border of the Latina Valley, a NW-SE trending piggyback basin formed in upper Miocene [*Cipollari and Cosentino*, 1993], partly reactivated with extensional motions during Plio-Quaternary [*Acocella et al.*, 1996]. The Plio-Quaternary structure of the area is mostly characterized by NW-SE trending normal faults, bordering the NE part of the Latina Valley and separating the upper Miocene-Quaternary sedimentary and volcanic deposits, within the Valley, from the Cretaceous and middle Miocene limestones [*Cavinato et al.*, 1993]. Field work in the Alatri area was thus focused along this NW-SE trending border fault system (Figure 6). The faults, mostly measured within Cretaceous limestones and upper Miocene sedimentary deposits, crosscut the upper Miocene compressive structures [*Cavinato et al.*, 1993], suggesting Pliocene-Quaternary activity. The collected structural data and their locations are displayed in Figure 6. The data consist of NW-SE and subordinate NE-SW faults associated with tectonic breccias, with a mean displacement of several tens of meters.

[22] While in the Fondi area the NE-SW systems (map in Figure 6) constitute ~55% of the Quaternary faults (total length ~60 km), in both the GDR Basin and the Alatri area the frequency of the NE-SW systems lowers to 14% (total length of 5–6 km). The map in Figure 6 also shows that across the margin, the control of the NE-SW structures on morphology sharply decreases toward NE. Despite the sharp NE decrease of the NE-SW systems, the extent and frequency of the NW-SE systems remain quite constant. These are in fact widespread and show a similar control on the morphology, bordering NW-SE basins, even though their estimated throw decreases toward NE [*Acocella et al.*, 1996, and references therein]. Recent structural studies in southern Latium suggests that north of the GDR Basin, Plio-Quaternary extension is moderate (5–15%), whereas

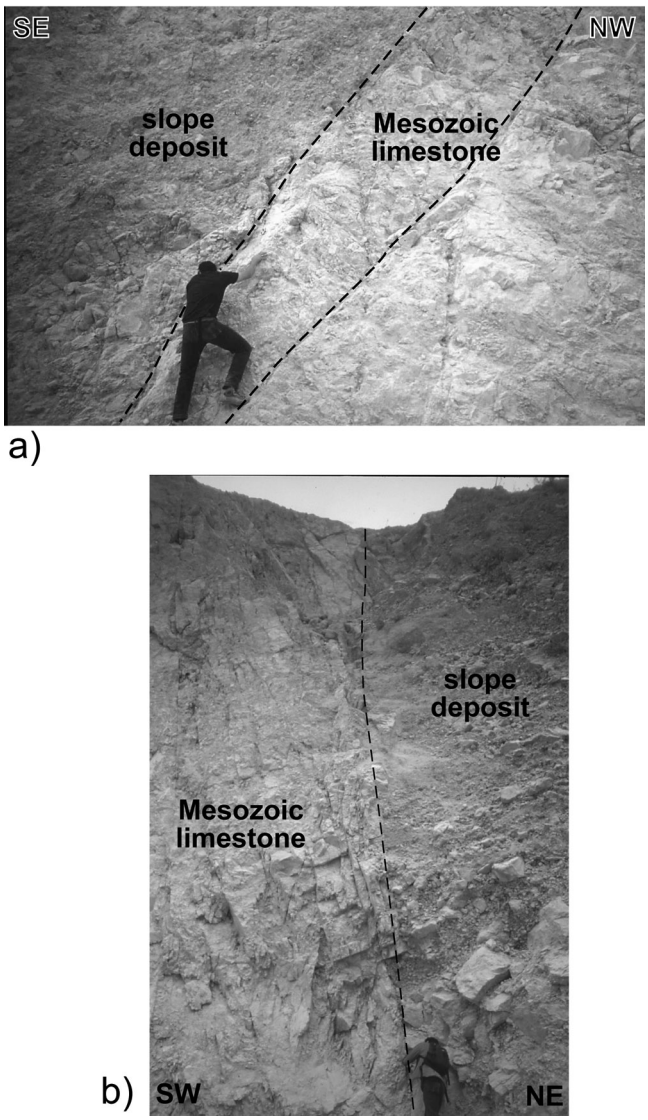

Figure 8. Fault systems on the NE edge of the Campania plain: (a) NE-SW trending fault juxtaposing Mesozoic limestones with upper Pleistocene slope deposit; and (b) NW-SE trending fault juxtaposing Mesozoic limestones with upper Pleistocene slope deposits. Displacement is of several tens of meters in both cases.

this is inferred to become much more significant to the SW [*Sani et al.*, 2004].

[23] The geometric and kinematic features of the fault systems in southern Latium (Fondi, GDR, and Alatri areas) are discussed in section 4.2.

4.1.2. NE Campania Plain

[24] The Campania Plain (southern Italy) is a NW-SE trending graben-like structure bordered by Mesozoic carbonate platforms, which subsided up to 5 km during the Plio-Quaternary (Figure 7) [*Carrara et al.*, 1973; *Finetti and Morelli*, 1974; *Fedi and Rapolla*, 1987]. The overall structure of the Plain, inferred from remote sensing, field, magnetic, gravity and seismic data [*Acocella et al.*, 2004, and references therein; *Bruno et al.*, 2004; *Piochi et al.*, 2005, and references therein], is shown in Figure 7. Most of the known and inferred fault systems in the Campania Plain have a NE-SW and NW-SE trend; these faults are responsible for the significant downthrown of the Mesozoic carbonates below the Plain. In particular, the continuity of the widespread NW-SE systems is interrupted by the NE-SW structures at the border (Monte Massico, Monti Lattari, Figure 7) and inside the Plain (areas of the Campi Flegrei and Somma-Vesuvio districts) (Figure 7). A major swarm of NE-SW structures inside the Plain, mostly revealed by geophysical data, is located along the Campi Flegrei Caldera and the volcanic islands of Procida and Ischia [*Carrara et al.*, 1973; *Rapolla et al.*, 1989; *Acocella et al.*, 2004; *Piochi et al.*, 2005, and references therein]. Its surface expression, in the Neapolitan volcanic area, is characterized by NE-SW trending faults, extensional fractures and dikes, as well as by the alignment of eruptive vents. The investigated area, in the NE portion of the Campania Plain, is located on the NE continuation of these transverse systems, where the Quaternary deposits of the Plain are juxtaposed to the Mesozoic limestones (Figure 7). Here NE-SW, NW-SE and subordinate E-W trending faults are outcropping, separating the limestone from Quaternary slope deposits. The stratigraphic position of these slope deposits with regard to dated volcanic products from the Campi Flegrei District suggests that the former have an age of 100–120 ka [*Acocella et al.*, 2003], implying an upper Pleistocene age for the faults within them. The mean displacement of these fault systems is a few tens of meters (Figure 8).

[25] Several NW-SE faults are found at this location; even though these have a strike which is not consistent with the local geomorphology (Figure 7 inset), the faults are parallel to the NW-SE margin of the Campania Plain (Figure 7). Therefore they may be considered as representative of the Quaternary faults bordering the NE margin of the Plain. Conversely, the observed NE-SW faults may be considered, for location and orientation, as the NE continuation of the transverse systems present along the Ischia-Campi Flegrei volcanic zone. The general geometric and kinematic features of these faults systems are discussed in section 4.2.

4.2. Geometry and Kinematics

[26] The faults zones measured at the areas of southern Latium and Campania Plain outcrop widely in large quarries and are associated with cataclastic breccia; when evaluated, their minimum displacement is in the order of tens of m. Therefore these faults are interpreted as forming large structures, representative of the Quaternary (except for the Alatri structures, of Pliocene-Quaternary age) regional setting of the margin.

[27] Both the NE-SW and the NW-SE faults in the areas of southern Latium and Campania Plain are arranged in parallel segments, and usually similarly dipping; the frequent uniform and moderate tilt of the layers within (opposite to the dip of the faults) highlights a domino-like style of faulting, at the scale of 10^1–10^2 m.

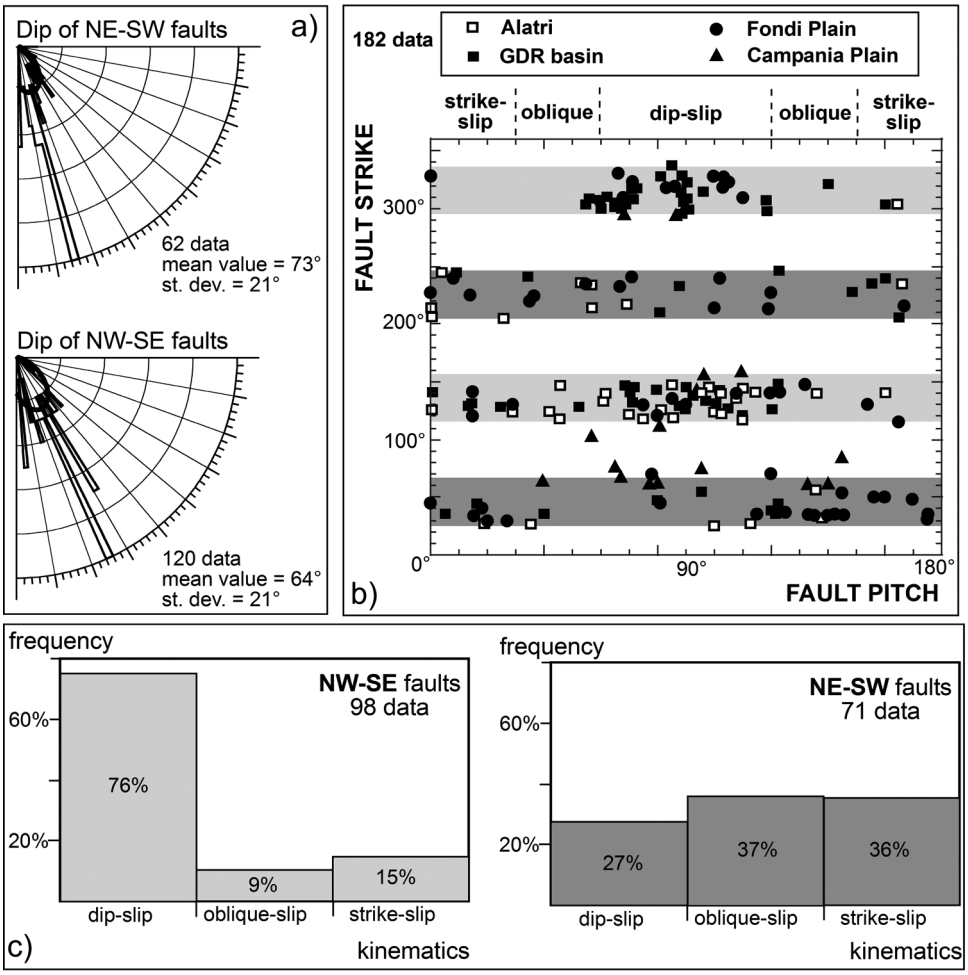

Figure 9. (a) Variation in dip of the (top) NE-SW and (bottom) NW-SE faults shown in Figures 6 and 7. (b) Variation of pitch values of the faults as a function of their strike (the dip direction of a fault is 90° larger than its strike). Lighter and darker grey horizontal bars are shown as reference for the NW-SE trend (135° ± 20° and 315° ± 20°) and the NE-SW trend (45° ± 20° and 225° ± 20°), respectively. (c) Frequency distributions of the (left) NW-SE and (right) NE-SW faults as a function of their dip-slip, oblique-slip, and strike-slip kinematics.

[28] The dip values of the NE-SW and NW-SE trending faults measured in the areas of southern Latium and Campania Plain are shown in Figure 9a. The mean dip of the NE-SW faults (73°) is similar to that of the NW-SE faults (64°).

[29] The kinematics of these faults is shown in Figure 9b, where the pitch of the fault is reported as a function of the fault strike. The data have been divided as a function of their location; in particular, the data relative to the area of southern Latium are divided for the Fondi Plain, GDR and Alatri areas. Lighter and darker grey horizontal bars are shown as reference for the NW-SE trend (135° ± 20° and 315° ± 20°) and the NE-SW trend (45° ± 20° and 225° ± 20°), respectively.

[30] It can be observed from the diagram that while most (76%) of the NW-SE faults have a dip-slip motion (60° < pitch < 120°), the majority (73%) of the NE-SW faults displays oblique to strike-slip motions (pitch < 60° and pitch > 120°). In particular, as far as the NW-SE faults are concerned, the faults dipping toward NE (uppermost horizontal grey bar) display, with few exceptions, dip-slip motions, whereas several faults dipping toward SW (third horizontal grey bar from above) display oblique motions.

[31] To highlight the kinematic features of Figure 9b, the kinematic distribution of the NW-SE (Figure 9c, left) and NE-SW (Figure 9c, right) faults is summarized in Figure 9c. The NW-SE faults with dip-slip motions (60° < pitch < 120°) are 76%; the NW-SE faults with oblique-slip motions (30° < pitch < 60° and 120° < pitch < 150°) are 9%; the NW-SE faults with strike-slip motions (0° < pitch < 30° and 150° < pitch < 180°) are 15% (Figure 9c). Conversely, the NE-SW faults with dip-slip motions (60° < pitch < 120°) are 27%; the NE-SW faults with oblique-slip motions (30° < pitch < 60° and 120° < pitch < 150°) are 37%; the NE-SW faults with strike-slip motions (0° < pitch < 30° and 150° < pitch < 180°) are 36% (Figure 9c). In general, Figure 9 indicates that the NW-SE systems mainly consist of high angle normal faults, whereas most of the

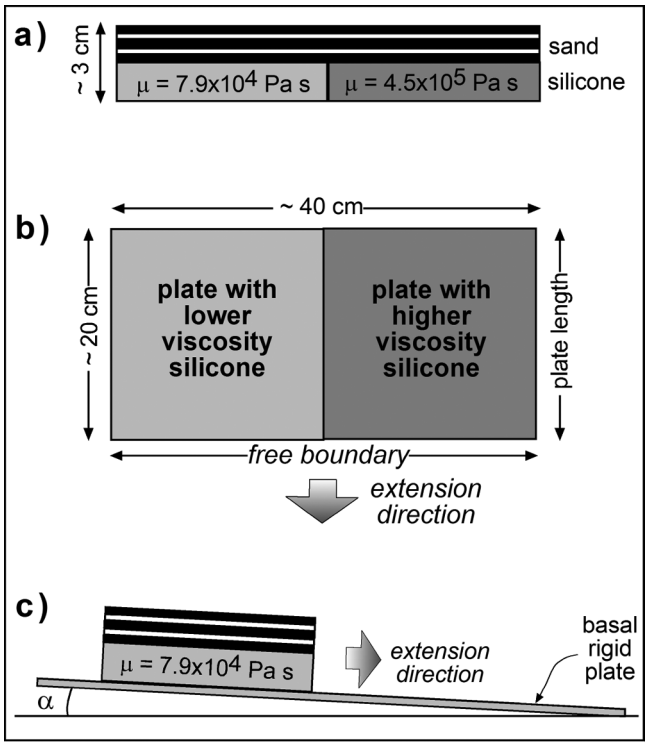

Figure 10. Sketch of the experimental apparatus of the analogue models. (a) Frontal section view; (b) map view; and (c) lateral section view. Modified after *Acocella et al.* [2005a] with permission from Elsevier.

high angle to subvertical NE-SW systems are transtensive, characterized by a significant left-lateral or right-lateral component of shear.

5. Results From Analogue Models

[32] In order to better understand the meaning of the deformation pattern observed on the Tyrrhenian margin of central Italy, previous [*Acocella et al.*, 2005a] analogue experiments were used. These aimed (1) to simulate the extensional evolution of the crust of the Tyrrhenian margin, characterized by orthogonal structures, with predominant normal (NW-SE systems) and transtensive (NE-SW systems) motions and (2) to define, through such a simulation, the possible conditions leading to the formation of transverse transtensive systems within an extensional context. A more detailed description of the experiments is reported by *Acocella et al.* [2005a].

[33] The extending crust of the Tyrrhenian margin has been simulated in its brittle and ductile components. The magmatic processes accompanying extension have not been taken into account; in fact, since the aim of the experiments is the definition of the conditions leading to the formation of the transverse structures of the extensional margin, the simulation of a magmatic component is not required. Moreover, experiments considering the conditions of emplacement of magma within extensional transfer zones have been previously done [*Corti et al.*, 2002, 2004].

[34] The considered parameters imposed in our experiments are: the initial thickness of the crust and of its brittle and ductile portions, the amount of extension, the tectonic strain rate and the presence of differential extension of adjacent crustal portions. These parameters have been scaled accordingly to our knowledge of the values of their equivalent in the Tyrrhenian area. In particular, the overall thickness of the crust, as well as its brittle and ductile portions, are evaluated from geophysical data [*Nicolich*, 1989; *Valensise and Pantosti*, 2001]. The amount of extension and the tectonic strain rates have been previously estimated [*Faccenna et al.*, 1997] and are reported in section 5.1. The occurrence of differential extension along the margin [*Royden et al.*, 1987; *Patacca et al.*, 1990] was described in section 2. However, since no data are available for a quantification, we simulated a wide range of possible values (see section 5.1).

5.1. Experimental Procedure

[35] A detailed description of the scaling procedure is reported by *Acocella et al.* [2005a]. Accordingly with the imposed length ratio ($L^* = 10^{-6}$), density ratio ($\rho^* \sim 0.5$) and gravity ratio ($g^* = 1$) between model and nature, the stress ratio is $\sigma^* = \rho^* g^* z^* \sim 5 \times 10^{-7}$. Cohesion c has the dimensions of stress; assuming a Mohr-Coulomb criterion and natural cohesion $c \sim 10^7$ Pa, a material with $c \sim 5$ Pa is required to simulate the brittle crust of the Tyrrhenian area: for this purpose, we use dry sand, with $c \sim 0$ Pa. Silicone putty with Newtonian behavior simulates the ductile crust. To reproduce different amounts of extension, we use two adjacent silicone layers (viscosities of 7.9×10^4 Pa s and 4.5×10^5 Pa s; Figure 10). The more viscous silicone was obtained by adding Ba sulphate powder, with a similar density ($\sim$1310 kg/m^3) to that of the silicone; the less viscous silicone is a pure silicone.

[36] The following relation applies to Newtonian ductile materials [*Benes and Davy*, 1996]:

$$\sigma_1^* - \sigma_3^* = \mu^* \varepsilon^* \quad (1)$$

where μ^* and ε^* are the viscosity and the strain rate ratios between model and nature, respectively. Being $\sigma_1^* - \sigma_3^* \sim 5 \times 10^{-7}$, the μ^* and ε^* ratios have to be scaled accordingly. Considering the viscosities of silicone and the viscosity of the lower crust (10^{20}–10^{21} Pa s [*Ranalli*, 1995]), $\mu^* \sim 10^{-16}$ and, as a result (from (1)), $\varepsilon^* \sim 5 \times 10^9$. An extensional strain rate $\varepsilon_n \sim 10^{-15}$ s^{-1} has been inferred in the Tyrrhenian area [*Faccenna et al.*, 1997]; to have $\varepsilon^* \sim 5 \times 10^9$, an experimental strain rate $\varepsilon_m \sim 5 \times 10^{-6}$ s^{-1} is required. Being $\varepsilon^* = 1/t^*$, 1 s in our experiments corresponds to 2×10^{10} s in nature. Consequently, the mean duration of the experiments (200–300 min) corresponds to 7–11 Ma in nature, consistently with the duration of the ongoing extension along the margin.

[37] The experimental setup consists of a 1–2 cm thick sand layer, a 1–2 cm thick silicone layer (two adjacent silicone portions with different viscosities) and a basal plate (Figure 10); these values simulate the original thickness of the Tyrrhenian-Apennines area before extension [*Faccenna*

et al., 1997]. The silicone layer is confined on three sides and has a free boundary along the fourth side. Extension is obtained by means of a tilt (4° to 6°) of the basal plate toward the free boundary (Figure 10c). The flow of silicone induces the thinning and extension of the sand pack. As the silicone has different viscosities, it undergoes different flow velocities and therefore stretching. Since the amount of extension within the sand is proportional to the amount of stretching of the underlying silicone, this setup permits to simulate the interaction of adjacent upper crust sectors with differential extension. The use of silicone with different viscosities does not simulates different types of ductile crust, and is only meant to simulate a differential extension.

5.2. Experimental Results

[38] All the experiments are consistent with a similar evolution, summarized in Figure 11. Experiment 7 in Figure 11 has T_b = 1.5 cm, T_d = 2 cm, (T_b and T_d are the sand and the silicone thicknesses, respectively), silicone viscosities of 7.9×10^4 (left plate) and 4.5×10^5 Pa s (right plate). At t = 0′ (minutes) the experiment is undeformed (Figure 11a). The tilt of the rigid base induces the flowing of silicone and extension in the two plates. At t = 60′ several depressions form (Figure 11b). Their lateral termination along the contact between the adjacent plates is marked by relay ramps or accommodation zones. These consist of a broad deformed area, delimited by normal faults, whose strike is almost perpendicular to the extension direction, even though displaying arcuate shapes. At t = 200′ the depressions are wider and deeper (Figure 11c). The normal faults bordering these grabens now interact with different modalities. Far from the free boundary, the interaction still occurs through relay ramps. Near the free boundary, the normal faults bordering the grabens are interrupted by left-lateral faults subparallel to the extension direction (Figure 11d). The transition between these two interaction styles consists of a narrow zone with left-lateral faults oblique to the extension direction (Figure 11d). Increasing the extension, the experiment does not show significant differences.

[39] The mean percentages of extension measured for each plate during the experiment are given by:

$$\beta_m = (L_m - L_i)/L_i$$

where L_i is the initial length of the plate and L_m is its incremental length at a given time; these percentages represent average values for each plate. The displacement vectors due to the extension of the reference grid along the plates contact (t = 300′) show that the differential extension increases toward the free boundary (Figure 11e). The percentages of extension (β_1 and β_2) related to each couple of nodes (origin of the dotted arrows) at the border between the plate contact are given, for each node, by (Figure 11e)

$$\beta = (L_f - L_i)/L_i$$

where L_i is the initial length of the model and L_f is the incremental length of the node plus the initial length of the model L_i. The difference ($\beta_1 - \beta_2$) between the percentages of extension for each couple of nodes at the sides of the contact gives the local percentage of differential extension $\Delta\beta$ (Figure 11e). The shades of grey show that the left-lateral faults connecting the two extending plates are limited to a differential extension $\Delta\beta > 24\%$ (Figure 11e). Below this threshold, the extending plates are connected by relay ramps. The differential extension of 24% represents therefore, in this experiment, the threshold between two types of interaction among extensional structures, characterized by relay ramps and transtensive faults. This behavior is a direct consequence of the relative (differential) extension, rather than the absolute values of extension.

[40] The remaining experiments show a deformation pattern similar to experiment 7, given by relay ramps far from the free boundary and strike-slip faults near to the boundary. The values of differential extension associated to the presence of strike-slip faults parallel to the extension direction in all the experiments give a mean threshold of 21% ± 3% [*Acocella et al.*, 2005a].

[41] Some basins on the plate with lower viscosity silicone appear, at the detailed scale, significantly stretched, resembling core complexes analogues (Figure 11c). However, despite these possible local variations, it has been demonstrated that the overall amount of extension along the length of each plate increases uniformly toward the free boundary, displaying a general constant behavior [*Acocella et al.*, 2005a].

6. Discussion

6.1. Definition of the Transverse Systems in Experiment and Nature

[42] The collected structural data in southern Latium and Campania Plain refer to a minor portion of the Tyrrhenian margin and any general interpretation should take into account for this limitation. However, multiple evidence suggests that the collected data may be useful in understanding the Quaternary tectonic evolution of the margin. In fact, the structural data collected in the areas of southern Latium and Campania Plain are characterized by the fol-

Figure 11. Evolution of analogue experiment 7 (modified after *Acocella et al.* [2005a] with permission from Elsevier). Map views of (a) undeformed stage; (b) experiment at t = 60′; (c) experiment at 200′; (d) enlargement of the plate contact area at 200′: transition from relay ramps, strike-slip faults oblique to the extension direction and strike-slip faults subparallel to the extension direction; and (e) enlargement of the plate contact area at 300′: displacement vectors of the nodes of the reference grid. The initial position of the nodes coincides with the origin of the arrows; β_1 and β_2 are the percentages of extension related to each couple of nodes (origin of the dotted arrows) at the two sides of the plate contact. The difference between the percentages of extension for each couple of nodes (origin of the dotted arrows) at the sides of the contact gives the percentage of differential extension $\Delta\beta$, represented as shades of grey.

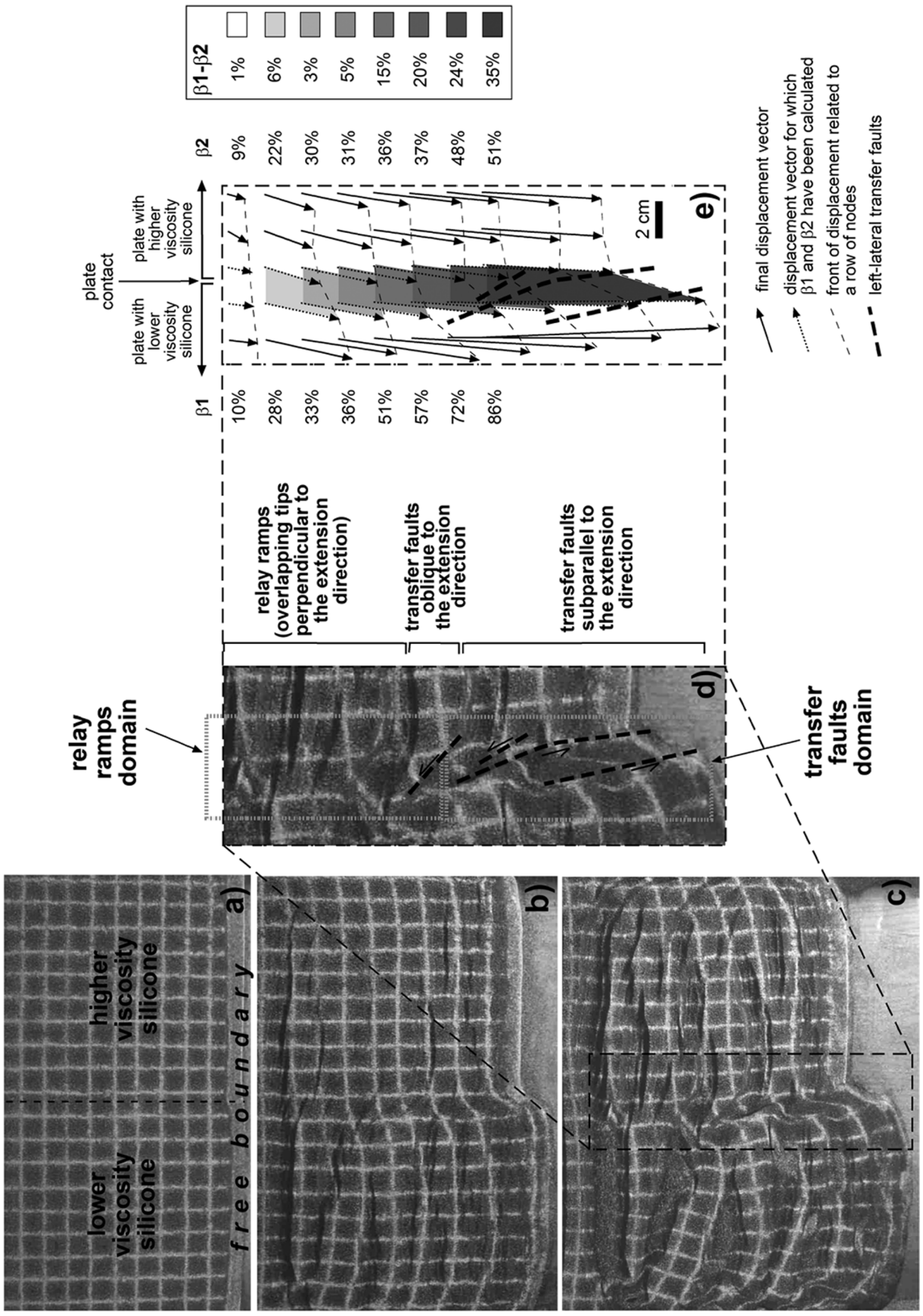
a)
b)
c)
d)
e)
lower viscosity silicone
higher viscosity silicone
free boundary
relay ramps domain
transfer faults domain
plate contact
plate with lower viscosity silicone
plate with higher viscosity silicone
β1
β2
β1-β2
10% 9% 1%
28% 22% 6%
33% 30% 3%
36% 31% 5%
51% 36% 15%
57% 37% 20%
72% 48% 24%
86% 51% 35%
relay ramps (overlapping tips perpendicular to the extension direction)
transfer faults oblique to the extension direction
transfer faults subparallel to the extension direction
2 cm
final displacement vector
displacement vector for which β1 and β2 have been calculated
front of displacement related to a row of nodes
left-lateral transfer faults

Figure 11

lowing important features: (1) are associated to first-order morphological features along the margin; (2) appear to be mostly Quaternary in age, coeval to most volcanoes; (3) have minimum displacements in the order of tens of m; (4) are outside the volcanic areas; and (5) permit to appreciate any structural variation across the margin (southern Latium transect). These features suggest that the measured NE-SW and the NW-SE faults are major structures, largely active during Quaternary. Moreover, the geometry, kinematics and age of the studied structures is consistent with what is known (see sections 2 and 3) for the other NW-SE and NE-SW structures along the margin. For these reasons, we suggest that the structural features of the studied systems in southern Latium and the Campania Plain may be representative of the overall Quaternary tectonic setting of the margin.

[43] The collected structural data on Quaternary faults show that while the NW-SE systems mainly consist of normal faults, the NE-SW faults are mostly transtensive; both fault systems have a similar overall high dip (Figure 9). The frequency of NE-SW faults across the margin decreases significantly toward the Apennines, becoming negligible immediately to the NE of the volcanic chain. This can be observed both at the large scale, along the margin (Figure 3), and at a detailed scale, across the margin, in southern Latium (Figure 6). The area of sharp decrease of NE-SW structures corresponds to a stretching factor $\beta \sim 1.3$ (Figures 12a and 2). To the NE, relay ramps and accommodation zones are the dominant type of interaction among NW-SE normal faults (Figure 12a) [*Morewood and Roberts*, 2000, and references therein].

[44] Results from balanced cross sections (Figure 2) suggest that in southern Latium, this transition zone with $\beta \sim 1.3$ lies along the Latina Valley (Figure 12a). *Sani et al.* [2004] suggest that here the stretching may be ~1.15, increasing significantly immediately to the south of the GDR Basin. Despite these possible minor discrepancies, both data sets point out to a significant variation in a limited area, the Latina Valley-GDR Basin. Also, the fact that few NE-SW faults are still observed to the north (Alatri area) suggests that the transition area, where $\beta \sim 1.3$, is broad and the dashed line in Figure 12 has to be considered, at least locally, a simplification of this transition zone.

[45] The analogue models have been performed to simulate the upper Miocene-Quaternary crustal extension along the Tyrrhenian margin, aiming at defining the modalities of formation of the transtensive transverse structures within an extensional context. The models show that transverse transtensive structures form only imposing a certain amount of differential extension. In particular, transverse transtensive structures form only when the differential stretching between two adjacent extending plates is large enough ($\Delta\beta > 21\%$). If the extension is not significant ($\Delta\beta < 21\%$), the interaction between nearby extensional structures occurs through relay ramps or accommodation zones (Figure 11b). The transition between these two behaviors consists of a narrow zone with strike-slip faults oblique to the extension direction (Figure 11d). This deformation pattern suggests that relay ramps, usually characterized by a moderate component of strike slip, accommodate minor differential displacements between adjacent extensional structures. Conversely, larger differential displacements are accommodated by predominant strike-slip systems, at first oblique (transition zone) and then parallel to the extension direction. The minor scatter (21% ± 3%) of the threshold in the various experiments suggests that the variations in the imposed parameters (ratio between the thickness of the brittle and ductile materials, the slope angle and the lateral dimensions of the models) do not significantly affect the modalities of deformation, the types of interaction and their threshold value [*Acocella et al.*, 2005a]. Therefore the main result of the experiments is that transtensive transverse structures can form within an extensional context only for certain values ($\Delta\beta < 21\%$) of differential extension.

[46] The experimental results have an important application to the structural setting of the Tyrrhenian margin, where the occurrence of differential extension has been previously highlighted (section 2). Even though no information is available on the amount of differential extension along the margin, it is noteworthy that transverse transtensive structures on the margin are observed for $\beta > 1.3$. It is evident that significantly lower values of extension (such as those found on the Apennines side of the margin) may not permit to have a differential extension $\Delta\beta > 21\%$. Conversely, values of extension $\beta > 1.3$ (such as those found on the Tyrrhenian side of the margin) may reasonably permit to locally achieve values of differential extension $\Delta\beta > 21\%$, developing transtensive transverse structures, such as the NE-SW systems observed along the margin. Therefore, for $\beta > 1.3$, both the field and the experimental data show the coexistence of normal faults responsible for extension and transtensive structures, subparallel to the extension direction. Conversely, for $\beta < 1.3$, both the field and the experimental data show that the differential extension, and therefore the interaction between extensional structures, is accommodated by relay ramps or accommodation zones. Such a consistency is also found in the transition zone, characterized, in the experiments, by strike-slip structures oblique to the extension direction and, on the margin, by N-S trending dextral faults (Sabina Fault, Latina Valley Fissure [*Alfonsi et al.*, 1991; *Acocella et al.*, 1996; *Sani et al.*, 2004]), immediately to the NE of the NE-SW structures domain (Figure 12a). In addition to previous interpretations of the N-S structures as lithospheric systems able to channel deep melts to the surface [*Sani et al.*, 2004], these N-S dextral faults may be therefore related to the larger amount of extension of the southern Tyrrhenian area.

[47] The interaction styles of the extensional structures observed on the Tyrrhenian margin and in the experiments thus appear qualitatively and quantitatively consistent. Both the experiments and the data along the margin show in fact distinct features as a function of the amount of differential extension: relay ramps, under lower differential extension, strike-slip faults, subparallel to the extension direction, under higher differential extension, and strike-slip faults, oblique to the extension direction, in the transition area. This similarity allows to interpret the overall pattern of the extensional structures in the central Apennines, as well as

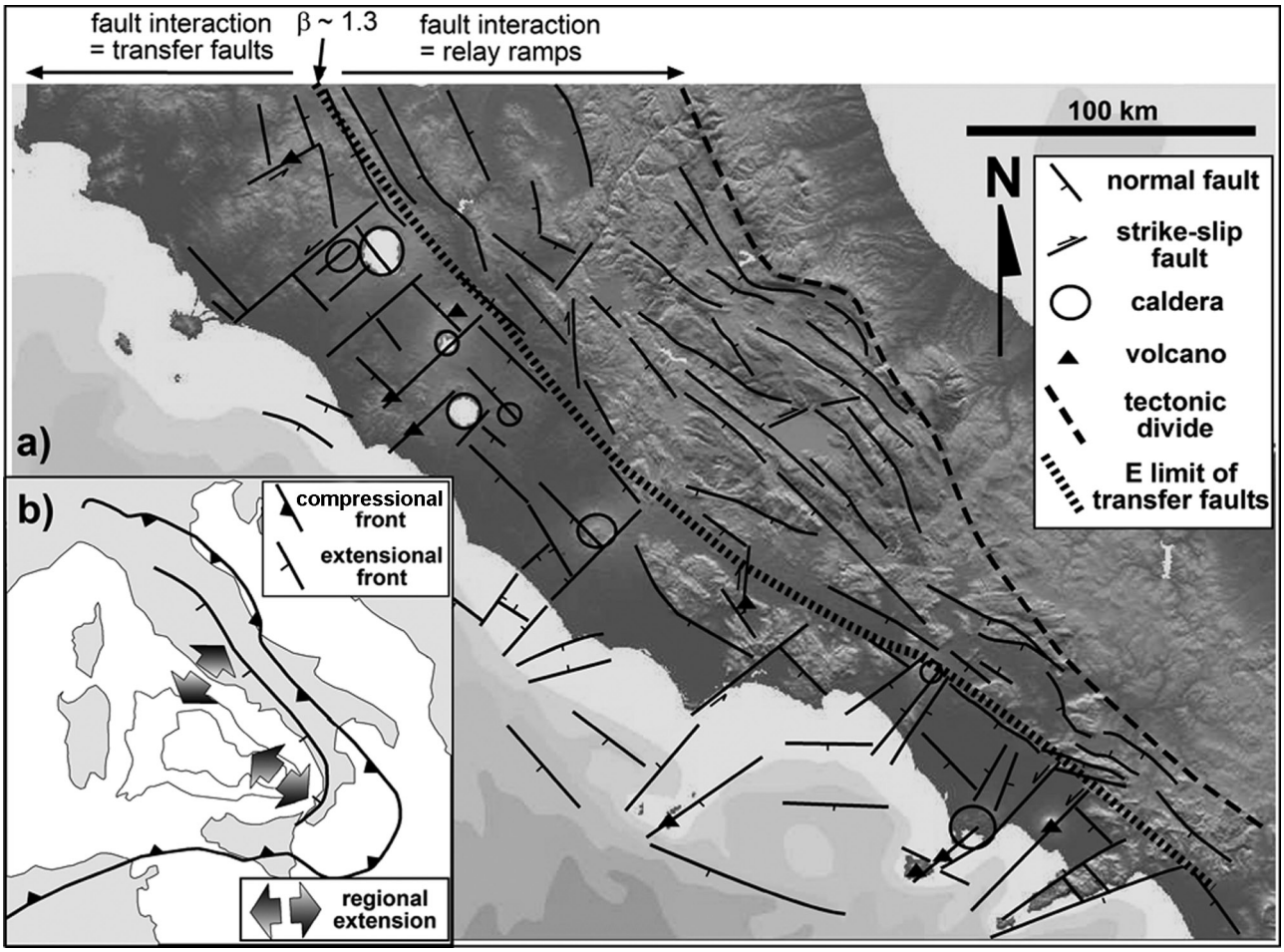

Figure 12. (a) Simplified structural map of central Italy to the west of the tectonic divide (that is the current limit between areas in compression and areas in extension), in the extensional domain. Dotted line shows the transition (corresponding to a stretching factor $\beta \sim 1.3$) between an area where the interaction among normal faults is characterized by transverse faults (to the west) and an area where the interaction is characterized by relay ramps or accommodation zones (to the east). (b) Simplified tectonic sketch of the Italian peninsula, showing the arcuate subduction front and, to the back, the main extension directions due to slab retreat. As a result, the northern Tyrrhenian margin is mainly characterized by NE-SW extension and the southern Tyrrhenian margin by NW-SE extension.

their different modalities of interaction, as due to the β increase and the related variations in the differential extension (Figure 12a).

[48] Because of their geometric and kinematic features, these transverse transtensive faults on the margin and in the experiments may be largely be interpreted as transfer systems of the normal faults, consistently with their kinematic role in the evolution of extensional domains [*Gibbs*, 1984, 1990]. Different evidence permits to interpret the NE-SW systems as transfer faults of the NW-SE normal faults: (1) their orthogonal orientation; (2) their coeval activity; (3) their kinematics; and (4) the frequency of the NE-SW structures across the margin, with a threshold ($\beta \sim 1.3$) explainable by the experimental data. The interpretation of the NE-SW structures along the margin as transfer faults is consistent with previous interpretations [*Liotta*, 1991; *Faccenna et al.*, 1994a; *Acocella et al.*, 1999].

[49] The NE-SW faults mostly display transtensive motion, which is both left- and right-lateral. This apparently contradictory kinematics is explained by the fact that adjacent crustal portions may undergo both dextral and sinistral shearing, depending on their location along the transfer fault with regard to the acting normal faults [*Gibbs*, 1984]. However, 27% of the transfer faults are characterized by dip-slip (normal) motions. In many cases, the dip-slip component develops transverse extensional basins, whose amount of subsidence is usually of very few kilometers [*Mariani and Prato*, 1988; *Faccenna et al.*, 1994a; *Berrino et al.*, 1998]. In a similar way, 24% of the NW-SE faults display oblique to strike-slip motions. The minor dip-slip motions on NE-SW faults and the oblique to strike-slip motions on NW-SE faults do not easily reconcile with the proposed model and additional factors have to be taken into account. One possibility is that the variable kinematics of

the NW-SE and NE-SW systems is related to the reactivation of preexisting compressional structures, such as NW-SE thrusts and NE-SW tear faults [*Faccenna et al.*, 1995; *D'Agostino et al.*, 1998; *Ghiestti and Vezzani*, 1997, 1999]). However, such a reactivation, when generating NW-SE strike-slip faults and NE-SW normal faults, has to take into account for the presence of minor stress variations along the margin. In this frame, a possibility to explain the observed kinematic variations is to consider the effect of the Quaternary southeastward retreat of the slab of oceanic lithosphere subducting below the Calabrian arc (Figure 12b). The NW-SE oriented extension related to the slab retreat (since middle Miocene [*Faccenna et al.*, 2001]) has been responsible for the development of the south Tyrrhenian basin, with higher rates of deformation (5 cm/yr) than those inferred for the north Tyrrhenian basin (2 cm/yr [*Patacca et al.*, 1990; *Turco and Zuppetta*, 1998]). The south Tyrrhenian basin started to develop, as a result of back-arc extension, since upper Miocene, as suggested by studies on extensional basins along the western Calabrian coast [*Mattei et al.*, 2002]. This process has been continuing until present, with the development of NE-SW trending Quaternary basins, associated with an overall NW-SE extension direction, along the Tyrrhenian coast of Calabria [*Patacca et al.*, 1990; *Monaco et al.*, 1997; *Monaco and Tortorici*, 2000]. In this frame, the minor kinematic variations observed in the NW-SE and NE-SW faults along the Tyrrhenian margin of central Italy can be interpreted as the effect of this significant extension (NW-SE oriented) associated with the slab retreat in the southern Apennines (Figure 12).

[50] This scenario is supported by (1) laboratory experiments, showing that the extended area behind a retreating slab is equivalent to the slab depth [*Funiciello et al.*, 2003]; in the Tyrrhenian case, the ~670 km deep slab may influence the extension in the north Tyrrhenian area, consistently with the fact that the northernmost transverse basin on the margin is found at the Vulsini District, at ~650 km from the slab (Figure 1); (2) bathymetric data, showing NE-SW trending ridges in the central southern Tyrrhenian Sea [*Gamberi and Marani*, 2004]; (3) numerical simulations, highlighting the effect of the NW-SE extension in the south Tyrrhenian Sea [*Bassi and Sabadini*, 1994]; and (4) borehole breakout data, consistent with a NE-SW extension direction along the margin [*Montone et al.*, 1999]; however, in the southern portion of the margin, a minor NW-SE direction of S_{hmin} (least horizontal stress) is repeatedly measured [*Amato and Montone*, 1997].

[51] The proposed tectonic model (Figure 12) explains the development of the coeval and variously oriented structures (NW-SE, NE-SW, and N-S) along the margin within a back-arc extension setting. In fact, the local structural variations, including the Quaternary NE-SW, NW-SE, and N-S strike-slip faults [*Marra*, 2001; *Sani et al.*, 2004; *Piochi et al.*, 2005] are here interpreted as the result of orthogonal extension to the back of the arcuate thrust front of the Apennines (Figure 12).

[52] Despite the possible control of the processes in the southern Tyrrhenian area, no evident strain gradient, associated to the NW-SE extension, is observed along the margin. This is suggested by the quite regular distribution of the transverse basins, implying a substantial uniform amount of NW-SE extension along the margin. The lack of a clear strain gradient may be explained by the fast SE migration of the Ionian slab, which allows quite consistent kinematic conditions along the margin.

[53] The reactivation of preexisting NE-SW faults (formed as lateral ramps or tear faults in the compressional phase) as transfer faults during extension is a likely possibility in the polyphased tectonic history of the Apennines [*Faccenna et al.*, 1995; *D'Agostino et al.*, 1998, and references therein]. As a consequence, the reactivation of the NE-SW faults may occur also for lower values of differential stretching than predicted ($\Delta\beta < 21\%$). The experimental threshold has thus to be considered as an uppermost limit.

6.2. Relationships Between NE-SW Systems and Volcanism

[54] Despite the width of the portion of the Tyrrhenian margin characterized by the presence of NW-SE and NE-SW structures (Figure 12a), the Plio-Quaternary volcanoes are mainly aligned along a narrow NW-SE belt. It is proposed that such a focusing of volcanic activity across the margin is the result of subcrustal dynamics, related to the selected rise of melts above the subducting slab. At a detailed scale, the structural data from the volcanic areas show that (1) the main volcanic edifices are located at the intersection among NE-SW (predominant) and NW-SE (subordinate) fault systems and (2) the eruptive fissures occur almost exclusively along NE-SW trending systems (Figure 5e).

[55] Two lines of evidence shows that transverse systems predate and control volcanic activity and should not be considered a mere effect of volcanism: (1) the onset of sedimentation within the transverse basins is 2–3 Ma older than the onset of volcanic activity and (2) transverse systems are coeval with the NW-SE structures responsible for the tectonic evolution of the margin that enhances the generation and uprise of magma.

[56] These considerations show that NE-SW structures locally control shallow magmatic processes along the Tyrrhenian margin. This control has to include the development of magma chambers, at the intersection among NW-SE faults and NE-SW structures, and the shallower uprise of magma, mostly in correspondence with transverse systems. Such a control occurs regardless of the compositional differences among the various volcanic districts. Results of analogue models of magma emplacement in extensional settings have also highlighted the importance of the accumulation of magma below extensional transfer zones [*Corti et al.*, 2002, 2004]. Within this frame, a twofold influence of the NE-SW transfer systems on volcanic activity is proposed, depending on their spacing and predominant kinematics.

[57] As far as the central volcanoes are concerned, these mostly lie at the intersection between NE-SW and NW-SE trending depressions. Central volcanoes consist of low-topography calderas and stratovolcanoes with summit calderas, the former usually showing higher erupted volumes

(Figure 3b). These two typologies may result from minor variations of a similar structural setting. Low topography calderas appear to be mainly controlled by widespread (delocalized) swarms of NE-SW and NW-SE trending structures, which allow larger magma storage in the crust, as well as its extrusion over a larger area; conversely, stratovolcanoes with summit calderas appear to be mainly controlled by focused (localized) swarms of NE-SW and NW-SE structures, allowing limited magma storage in the crust, focused below the conduit of a stratovolcano (Figure 4). These considerations are consistent with analogue models of magma emplacement, showing that focused deformation at surface enhances the localized rise of magma [*Corti et al.*, 2002].

[58] Three main processes may explain the accumulation of magma below both types of central volcanoes. In one case, the intersection between NE-SW and NW-SE structures increases the permeability of the crust and focuses the rise and emplacement of magmas. In the second case, the NW-SE normal faults along the volcanic chain are responsible for an overall crustal thinning of ~5 km (~1.5 kbar): of these, ~4 km are due to the westward shallowing of the Moho and ~1 km is related to the difference in topography [*Locardi and Nicolich*, 1988; *D'Agostino et al.*, 1998]. The multiple and widely spaced sets of NE-SW faults responsible for transverse basins also have a significant dip-slip component. An additional decompression associated to these structures can be roughly estimated, largely from topography differences, as ~1 km (~0.3 kbar). This further decompression (~20% of the one induced by NW-SE faults) is enough to locally enhance Rayleigh-Taylor instabilities [*Turcotte and Schubert*, 1982], inducing the selective uprise of magmas along the margin; this in turn enhances regularly spaced magma accumulation in the upper crust, developing shallow reservoirs and, consequently, the volcanoes at surface. Such a mechanism of decompression induced by the development of orthogonal basins plays a major role in enhancing the selected rise of magma along the margin, as also suggested by the larger erupted volumes (Figure 3b). The decompression associated with highly asymmetric basins (fault controlled on one side) may be significantly lower, as at the Fondi Plain, which lacks a volcanic edifice and shows magmatic activity only along the offshore continuation of its NE-SW trending border fault (Figure 3). A third mechanism is suggested by analogue models of magma emplacement in rift zones [*Corti et al.*, 2004, and references therein]; this mechanism does not require significant dip-slip transfer faulting and therefore is best applied to those central volcanoes where the decompression induced by the transverse basin may be too low to induce significant melting. Accordingly with the experimental results, the uprising magma in extensional settings may be subject to rift parallel migration toward the transfer zones by lateral pressure gradients generated by rifting at surface; these gradients may result in the accumulation of magma below transfer zones [*Corti et al.*, 2004].

[59] In the case of eruptive fissures, these are usually related to single sets of NE-SW structures (even though Ernici shows a major N-S fissure) with little or no evidence of significant dip-slip component of motion (Figure 3); In these cases, magma, in the form of dikes, may intrude the NE-SW (and, subordinately, N-S) structures because of (1) the drop in tensile strength along the fault planes, (2) their high angle to subvertical attitude and (3) the above mentioned along-rift lateral pressure gradients [*Corti et al.*, 2004]. In particular, point 2 can be appreciated in Figure 9a and is suggested by the kinematics of the collected structural data (Figure 9c) and by previously reported structural data [*Fazzini and Gelmini*, 1982; *Buonasorte et al.*, 1987; *Acocella et al.*, 1996]. Moreover, since strike-slip faults often form flower-like structures, it is likely that the dip of the NE-SW (and N-S) systems observed at surface increases at depth, conversely to what expectable from the NW-SE normal faults, often reactivating preexisting low-angle thrusts in the Apennines [*Faccenna et al.*, 1995; *D'Agostino et al.*, 1998]. Subvertical fractures can be penetrated more easily by magma than high angle normal faults [*Acocella et al.*, 1999]. At depths of very few km, the possibility to penetrate high angle or subvertical fractures also depends on their orientation with regard to the differential horizontal stress ($\sigma_{hmax} - \sigma_{hmin}$). Nevertheless, the difference in the required magmatic pressure p to penetrate subvertical faults and high angle normal faults increases with the depth z (Figure 13) [*Acocella et al.*, 1999]. Such a difference, at a certain depth, becomes larger than the differential horizontal stress [*Vigneresse*, 1995]; when this occurs (grey area in Figure 13), the possibility to intrude magma along a fracture becomes primarily controlled by its dip, rather than its direction with regard to the horizontal tectonic stresses. Also, for a given magmatic pressure, subvertical fractures can be tapped more deeply than normal faults, being potentially intruded by more mafic magmas and enhancing the emission of the primitive components [*Acocella et al.*, 1999]. This might explain the common association of NE-SW and N-S eruptive fissures with the most primitive magmas along the margin, such as at Latera, Ernici, Campi Flegrei, and Vesuvio.

[60] The collected data suggest that different structures control magma generation, uprise and emplacement at different crustal levels (Figure 14). The generation and uprise of magma to upper crustal levels is mainly controlled by the NW-SE normal faults, responsible for regional extension, crustal thinning, decompression and rise of the isotherms (Figure 14). Conversely, the uprise and emplacement of magma at upper crustal levels, as suggested by the structures associated with volcanic activity, is mainly controlled by transverse structures (Figure 14b). The specific modalities of such control depend largely on the kinematics of the NE-SW faults (Figure 14b insets), which, in turn, is influenced by the superimposed extension directions in the central and southern Tyrrhenian Sea. Therefore extension plays a twofold role, direct (through the NW-SE structures) and indirect (creating the NE-SW transfer structures associated to the NW-SE faults) on the rise and emplacement of magma along the Tyrrhenian margin.

[61] The control of different structures, acting at different crustal levels, on the generation, uprise and emplacement of

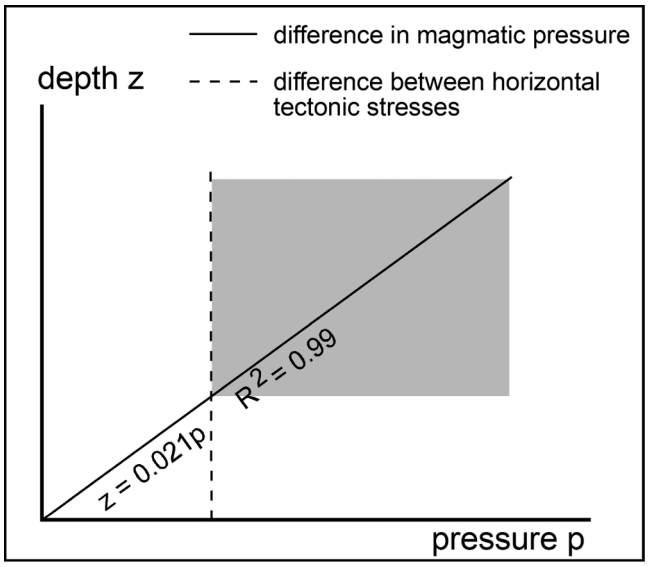

Figure 13. Difference in the magmatic pressures required to penetrate a subvertical (dip of 90°) and a high angle (dip of 60°) fracture (solid line) and difference between the horizontal tectonic stresses ($\sigma_{hmax} - \sigma_{hmin}$; dashed line) as a function of the depth of the fracture. Equation for solid line is derived from *Acocella et al.* [1999]; the vertical dashed line assumes no significant variation of the difference in the tectonic stresses with depth. Grey area shows the depth above which the penetration of a fault is mainly controlled by its dip, rather than its strike.

magma inferred for the Tyrrhenian margin has been previously proposed in other magmatic provinces. In the nearby Tuscan Magmatic Province (Figure 1), mostly characterized by intrusives, the rise and emplacement of Mio-Pliocene plutons has been controlled by different structures active in the lower and upper crust [*Acocella and Rossetti*, 2002]. In the Ethiopian Rift, the location of felsic calderas along the axis of the rift is controlled by reactivated prerift transverse structures [*Acocella et al.*, 2002]; also, the clustering of volcanoes at transfer zones along the Western Branch of the Eastern African Rift System is interpreted to be controlled by shallow transverse structures within an extensional context [*Acocella et al.*, 1999; *Corti et al.*, 2004]. Volcanism in the central Andes is similarly controlled by different structures acting at different crustal levels [*Riller et al.*, 2001; *Matteini et al.*, 2002; *Acocella et al.*, 2005b]. Volcanic activity along the transtensive Mexican Volcanic Belt is also controlled by transverse systems [*Tibaldi*, 1992; *Norini et al.*, 2005]. Even though these cases provide isolated spots in the frame of the global magmatic processes, it is noteworthy that a common mechanism may explain the rise of magma through the crust in different geodynamic settings, as at back arcs (Tyrrhenian margin, Tuscan Magmatic Province), continental rifts (Ethiopian Rift) and arcs (central Andes, Mexican Volcanic Belt). This common mechanism consists of the fact that while the extensional or the arc-parallel structures are responsible for the regional generation and rise of magma, the selective location of volcanoes is mainly related to the presence of transverse structures. Therefore the rise of magma through the crust seems to focus, along volcanic zones in extensional and compres-

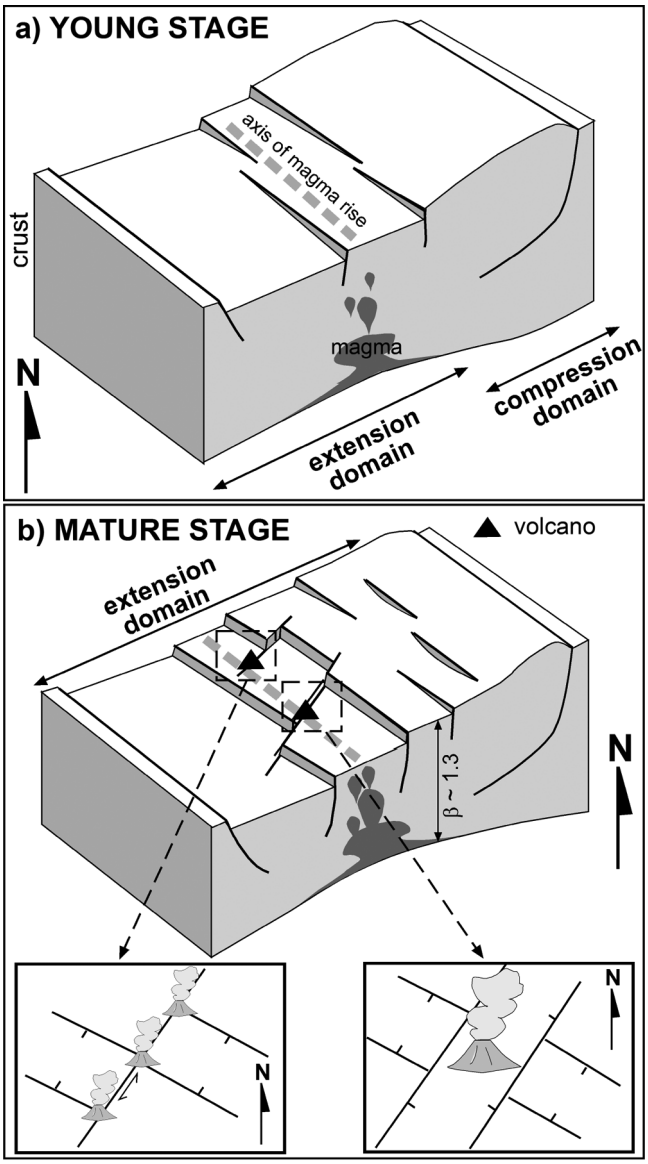

Figure 14. Structural control on magmatism along the Tyrrhenian margin of central Italy. (a) Early stage of evolution of the Tyrrhenian margin. Extension due to NW-SE normal faults is moderate and focused; the associated decompression allows the formation of a NW-SE trending area of partial melting in the lower crust. (b) Mature stage. Extension is more intense and widespread and has migrated to the present Apennines divide. Transfer faults form in the more stretched crust ($\beta > 1.3$), controlling the uprise and emplacement of magma at shallower crustal levels; to the east, the lower amount of extension hinders the development of transfer faults and fault interaction occurs by means of relay ramps. Insets show the twofold control of NE-SW structures on volcanism. Not to scale.

sional settings, at the intersection between the rift (or arc-parallel) structures and the transverse systems. Depending on their kinematics (strike-slip or extensional), these transverse systems may play different roles on the rise and emplacement of magma, as proposed for the Tyrrhenian margin. Where transverse structures are lacking, any local increase in extension along the rift may enhance volcanic activity, as proposed for the moderately oblique rifting along the Taupo Volcanic Zone, New Zealand [*Spinks et al.*, 2005].

7. Conclusions

[62] The agreement among the collected data suggests the following points.

[63] 1. The NE-SW transtensive structures along the margin are transfer faults of the NW-SE normal faults, developed within a significantly stretched ($\beta > 1.3$) crust, which allows sufficient differential stretching ($\Delta\beta > 0.21$). Where the stretching is lower ($\beta < 1.3$), relay ramps are the common type of interaction between normal faults in the Apennines; here the few NE-SW faults are due to the reactivation of preexisting faults. The transition between these two behaviors may coincide with the major N-S dextral faults to the NE of the volcanic axis.

[64] 2. The minor (<30%) NW-SE strike-slip faults and NE-SW normal faults measured on the margin are the result of the NW-SE extension due to the SE slab retreat beneath the Calabrian arc.

[65] 3. The proposed tectonic model (Figure 12) explains the development of the coeval and variously oriented structures (NW-SE, NE-SW, and N-S) along the margin as the result of orthogonal extension to the back of the arcuate thrust front of the Apennines.

[66] 4. The different stress conditions in the central (NE-SW extension) and southern (NW-SE extension) Tyrrhenian Sea, as well as the reactivation of preexisting compressional structures, can account for the composite (dip-slip to strike-slip) kinematics of the NE-SW structures, which, in turn, exerts a twofold role in controlling volcanism.

[67] 5. Where the dip-slip component of the transfer faults forms transfer basins, a local increase of ~20% in the regional decompression can occur. This results in the regularly spaced distribution of the main volcanic edifices, at the intersection among NW-SE normal faults and NE-SW transfer systems. Possible additional mechanisms to explain magma accumulation below transfer basins include along-rift lateral pressure gradients [*Corti et al.*, 2004].

[68] 6. Where the strike-slip component of the transfer faults is predominant, their subvertical attitude can enhance their permeability to magma, especially at moderate depths, accounting for the compositionally primitive NE-SW fissure eruptions. Possible additional mechanisms to explain magma accumulation below transfer faults include along-rift lateral pressure gradients [*Corti et al.*, 2004].

[69] 7. The Tyrrhenian margin provides therefore a case of twofold control of extension on volcanism. Even though NW-SE faults, related to regional extension, control the generation and uprise of magma (as shown by the alignment of volcanoes), NE-SW transfer structures control magma ascent and emplacement at shallower levels (as shown by the structural setting of single volcanoes). The fact that different structures control magmatism at different crustal levels has close similarities with other areas worldwide (Tuscan magmatic province, in Italy, East African Rift System, central Andes, Mexican Volcanic Belt).

[70] **Acknowledgments.** The authors are deeply indebted to P. Morvillo for performing the experiments and N. D'Agostino for Figure 11e. C. Faccenna and M. Mattei provided helpful discussions. L. Minore participated to the field work in the Campania Plain. M. Di Vito, G. Orsi, and G. Zanchetta provided expert field advice in dating deposits in the Campania Plain. B. Behncke reviewed an early version of the manuscript and improved the English. The authors thank the Associate Editors L. Ratschbacher and G. Bertotti, G. Corti, A. Gudmundsson, O. Merle, and two anonymous reviewers for their very constructive comments. Work was partly financed with GNV (Campi Flegrei Project) Funds. This is a contribution to project IGCP 455 (responsible A. Tibaldi).

References

Acocella, V., and R. Funiciello (1999), The interaction between regional and local tectonics during resurgent doming: The case of the island of Ischia, Italy, *J. Volcanol. Geotherm. Res.*, *88*, 109–123.

Acocella, V., and R. Funiciello (2002), Transverse structures and volcanic activity along the Tyrrhenian margin of central Italy, *Mem. Soc. Geol. Ital.*, *1*, 739–747.

Acocella, V., and F. Rossetti (2002), The role of extensional structures on pluton ascent and emplacement: The case of southern Tuscany (Italy), *Tectonophysics*, *354*, 71–83.

Acocella, V., C. Faccenna, and R. Funiciello (1996), Elementi strutturali della media Valle Latina, *Boll. Soc. Geol. Ital.*, *115*, 501–518.

Acocella, V., F. Salvini, R. Funiciello, and C. Faccenna (1999), The role of transfer structures on volcanic activity at Campi Flegrei (southern Italy), *J. Volcanol. Geotherm. Res.*, *91*, 123–139.

Acocella, V., A. Gudmundsson, and R. Funiciello (2000), Interaction and linkage of extensional fractures: Examples from the rift zone of Iceland, *J. Struct. Geol.*, *22*, 1233–1246.

Acocella, V., T. Korme, F. Salvini, and R. Funiciello (2002), The control of transverse tectonics on caldera development in the Ethiopian Rift, *J. Volcanol. Geotherm. Res.*, *119*, 189–203.

Acocella, V., R. Funiciello, L. Minore, G. Zanchetta, M. Di Vito, and G. Orsi (2003), Lateral continuation of the transverse structures at Campi Flegrei area, paper presented at the General Assembly of the National Group of Volcanology, Rome.

Acocella, V., et al. (2004), La struttura dell'area flegrea, paper presented at the Gruppo Nazionale per la Vulcanologia Meeting, Naples, Italy, Dec.

Acocella, V., P. Morvillo, and R. Funiciello (2005a), What controls relay ramps and transfer faults within rift zones? Insights from analogue models, *J. Struct. Geol.*, *27*, 397–408.

Acocella, V., A. Dini, A. Gioncada, H. Guillou, M. Matteini, R. Mazzuoli, R. Omarini, A. Uttini, and L. Vezzoli (2005b), The magmatism linked to the transversal structures in central Andes: The Tastil-Las Burras Complex (24°19′S, 65°50′E) NW Argentina, paper presented at the European Geophysical Union Assembly, Vienna, Austria, April.

Alfonsi, L., R. Funiciello, M. Mattei, O. Girotti, A. Maiorani, M. Preite Martinez, C. Trudu, and B. Turi (1991), Structural and geochemical features of the Sabina strike-slip fault (central Apennines), *Boll. Soc. Geol. Ital.*, *110*, 217–230.

Amato, A., and P. Montone (1997), Present-day stress field and active tectonics in southern peninsular Italy, *Geophys. J. Int.*, *130*, 519–534.

Anders, M. H., and R. W. Schlische (1994), Overlapping faults, intrabasin highs and the growth of normal faults, *J. Geol.*, *102*, 165–180.

Angelucci, A., G. Civitelli, P. Brotzu, L. Morbidelli, and G. Traversa (1974), Il vulcanismo pleistocenico delle media Valle Latina (Lazio). Caratteristiche petrografiche e geologiche dei principali affioramenti lavici, *Geol. Romana*, *13*, 83–123.

Antonioli, F., M. Frezzotti, and E. Valpreda (1990), Evoluzione geologica della Piana di Fondi e delle aree marginali durante il Quaternario, *Mem. Descr. Carta Geol. Ital.*, *XXXVIII*, 97–124.

Baldi, P., F. A. Decandia, A. Lazzarotto, and A. Calamai (1974), Studio geologico del substrato della copertura vulcanica laziale nella zone dei laghi di

Bolsena, Vico e Bracciano, *Mem. Soc. Geol. Ital.*, *13*, 575–606.

Barberi, F., G. Buonasorte, R. Cioni, A. Fiordelisi, L. Foresi, S. Iaccarino, M. A. Laurenzi, A. Sbrana, L. Vernia, and I. M. Villa (1994), Plio-Pleistocene geological evolution of the geothermal area of Tuscany and Latium, *Mem. Descr. Carta Geol. Ital.*, *XLIX*, 77–134.

Bassi, G., and R. Sabadini (1994), The importance of subduction for the modern stress field in the Tyrrhenian area, *Geophys. Res. Lett.*, *21*, 329–332.

Beccaluva, L., P. Di Girolamo, and G. Serri (1984), High-K calcalkalic, shoshonitic and leucitic volcanism of Campania (Roman Province, southern Italy): Trace elements constraints on the genesis of an orogenic volcanism in a post collisional extensional setting, report, pp. 1–47, Cursi, Pisa, Italy.

Benes, V., and P. Davy (1996), Modes of continental lithospheric extension: Experimental verification of strain localization processes, *Tectonophysics*, *254*, 69–87.

Berrino, G., G. Corrado, and U. Riccardi (1998), Sea gravity data in the Gulf of Naples: A contribution to delineating the structural pattern of the Vesuvian area, *J. Volcanol. Geotherm. Res.*, *82*, 139–150.

Boillot, G., M. O. Beslier, C. M. Krawczyk, D. Rappin, and T. J. Reston (1995), The formation of passive margin: Constraints from the crustal structure and segmentation of the deep Galicia margin, Spain, in *The Tectonics, Sedimentation and Palaeoceanography of the North Atlantic Region*, edited by R. A. Scrutton et al., *Geol. Soc. Spec. Publ.*, *90*, 71–91.

Bosi, V., and G. Giordano (1997), Stress field evolution in central Italy during middle-late Pleistocene: New information from southern Latium, *Quaternario*, *10*(2), 631–636.

Brun, J. P., F. Wenzel, and Ecors-Dekorp Team (1991), Crustal-scale structure of the southern Rhinegraben from ECORS-DEKORP seismic reflection data, *Geology*, *19*, 758–762.

Bruno, P. P., G. Cippitelli, and A. Rapolla (1998), Seismic study of the Mesozoic carbonate basement around Mt. Somma-Veusvius, Italy, *J. Volcanol. Geotherm. Res.*, *84*, 311–322.

Bruno, P. P., G. De Astis, and M. Piochi (2004), The influence of regional stress and magma production rates on the style of volcanism at Campi Flegrei and Somma-Vesuvio (Italy), paper presented at 1st European Geophysical Union Meeting, Nice, France.

Buonasorte, G., A. Fiordelisi, and U. Rossi (1987), Tectonic structures and geometric setting of the Vulsini Volcanic Complex, *Period. Mineral.*, *56*, 123–136.

Calamai, A., R. Cataldi, P. Squarci, and L. Taffi (1970), Geology, geophysics and hydrogeology of the Monte Amiata geothermal fields, *Geothermics*, special issue, 1–9.

Capaccioni, B., G. Nappi, A. Renzulli, and P. Santi (1987), The eruptive history of Vepe Caldera (Latera Vocano): A model inferred from structural and geochemical data, *Period. Mineral.*, *56*, 269–283.

Carmassi, M., D. De Rita, M. Di Filippo, R. Funiciello, and M. Sheridan (1983), Geology and volcanic evolution of the island of Ponza, Italy, *Geol. Romana*, *22*, 211–232.

Carrara, E., F. Iacobucci, E. Pinna, and A. Rapolla (1973), Gravity and magnetic survey of the Campanian volcanic area, southern Italy, *Bol. Geofis. Teorica Appl.*, *XV*, 39–51, 57.

Cavinato, G. P., S. Corrado, and M. Sirna (1993), Geometrie ed evoluzione cinematica del settore centrale della catena Simbruino-Ernica (Lazio, Appennino centrale), *Geol. Romana*, *29*, 435–453.

Cavinato, G. P., D. Cosentino, D. De Rita, R. Funiciello, and M. Parotto (1994), Tectonic-sedimentary evolution of intrapenninic basins and correlation with the volcano-tectonic activity in central Italy, *Mem. Descr. Carta Geol. Ital.*, *XLIX*, 63–76.

Cipollari, P., and D. Cosentino (1993), Le "Arenarie di Torrice": Un deposito di bacino di piggy back del Messiniano dell'appennino centrale, *Boll. Soc. Geol. Ital.*, *112*, 497–505.

Civetta, L., F. Innocenti, P. Manetti, A. Peccerillo, and G. Poli (1981), Geochemical characteristics of potassic volcanics from Mts. Ernici (southern Latium, Italy), *Contrib. Mineral. Petrol.*, *78*, 37–47.

Civetta, L., G. Gallo, and G. Orsi (1991), Sr and Nd isotope and trace element constraints on the chemical evolution of the magmatic system of Ischia (Italy) in the last 55 ka, *J. Volcanol. Geotherm. Res.*, *46*, 213–230.

Clemson, J., J. Cartwright, and J. Booth (1997), Structural segmentation and the influence of basement structure on the Namibian passive margin, *J. Geol. Soc. London*, *154*, 477–482.

Cordell, L. (1978), Regional geophysical setting of the Rio Grande Rift, *Bull. Geol. Soc. Am.*, *89*, 1073–1090.

Corti, G., M. Bonini, F. Mazzarini, M. Boccaletti, F. Innocenti, P. Manetti, G. Mulugeta, and D. Sokoutis (2002), Magma-induced strain localization in centrifuge models of transfer zones, *Tectonophysics*, *348*, 205–218.

Corti, G., M. Bonini, D. Sokoutis, F. Innocenti, P. Manetti, S. Cloetingh, and G. Mulugeta (2004), Continental rift architecture and patterns of magma migration: A dynamic analysis based on centrifuge models, *Tectonics*, *23*, TC2012, doi:10.1029/2003TC001561.

D'Agostino, N., N. Chamot Rooke, R. Funiciello, L. Jolivet, and F. Speranza (1998), The role of preexisting thrust faults and topography on the styles of extension in the Gran Sasso Range (central Italy), *Tectonophysics*, *292*, 229–254.

D'Agostino, N., R. Giuliani, M. Mattone, and L. Bonci (2001), Active crustal extension in the central Apennines (Italy) inferred from GPS measurements in the interval 1994–1999, *Geophys. Res. Lett.*, *28*, 2121–2124.

D'Antonio, M., L. Civetta, G. Orsi, L. Pappalardo, M. Piochi, A. Caradente, S. de Vita, M. Di Vito, R. Isaia, and J. Southon (1999), The present state of the magmatic system of the Campi Flegrei Caldera based on reconstruction of its behaviour in the past 12 ka, *J. Volcanol. Geotherm. Res.*, *91*, 247–268.

De Rita, D., and G. Giordano (1996), Volcanological and structural evolution of Roccamonfina volcano (Italy): Origin of the summit caldera, in *Volcano Instability on the Earth and Other Planets*, edited by W. J. McGuire, A. P. Jones, and J. Neuberg, *Geol. Soc. Spec. Publ.*, *110*, 209–224.

De Rita, D., R. Funiciello, and C. Rosa (1992), Volcanic activity and drainage network evolution of the Alban Hills area (Rome, Italy), *Acta Vulcanol.*, *2*, 185–198.

De Rita, D., R. Funiciello, L. Corda, A. Sposato, and U. Rossi (1993), Volcanic units of the Sabatini Volcanic complex, in *Sabatini Volcanic Complex*, edited by M. Di Filippo, pp. 33–80, Cons. Naz. delle Ric., Rome.

De Rita, D., et al. (1994a), Geological -petrological evolution of the Ceriti Mountains area (Latium, central Italy), *Mem. Descr. Carta Geol. Ital.*, *XLIX*, 291–322.

De Rita, D., A. Bertagnini, C. Faccenna, P. Landi, C. Rosa, F. Zarlenga, M. Di Filippo, and M. G. Carboni (1994b), Evoluzione geopetrograficastrutturale dell'area tolfetana, *Boll. Soc. Geol. Ital.*, *116*, 143–175.

De Rita, D., C. Faccenna, R. Funiciello, and C. Rosa (1995), Stratigraphy and volcano-tectonics of the volcano of the Alban Hills, in *The Volcano of the Alban Hills*, edited by R. Trigila, pp. 33–71, Cons. Naz. delle Ric., Rome.

De Rita, D., M. di Filippo, and C. Rosa (1996), Structural evolution of the Bracciano volcano-tectonic depression, Sabatini Volcanic District, Italy, in *Volcano Instability on the Earth and Other Planets*, edited by W. J. McGuire, A. P. Jones, and J. Neuberg, *Geol. Soc. Spec. Publ.*, *110*, 225–236.

De Rita, D., G. Giordano, and A. Cecili (2001), Submarine rhyolitic dome growth and evolution (Ponza, Italia), *J. Volcanol. Geotherm. Res.*, *107*, 221–239.

Di Filippo, M., and B. Toro (1980), Analisi gravimetrica delle strutture geologiche del Lazio meridionale, *Geol. Romana*, *19*, 285–294.

Di Girolamo, P., and G. Rolandi (1975), Vulcanismo sottomarino latitebasaltico-latitico (serie potassica) nel canale d'Ischia (Campania), *Rend. Accad. Sci. Fis. Maemat. Napoli*, *42*, 561–596.

Doglioni, C., F. Innocenti, C. Morellato, D. Procaccianti, and D. Scrocca (2004), On the Tyrrhenian Sea opening, *Mem. Descr. Carta Geol. Ital.*, *XLIV*, 147–164.

Dorè, A. G., E. R. Lundin, C. Fichler, and O. Olesen (1997), Patterns of basement structure and reactivation along the NE Atlantic margin, *J. Geol. Soc. London*, *154*, 85–92.

Duenbendorfer, E. M., and R. A. Black (1992), Kinematic role of transverse structures in continental extension: An example from the Las Vegas Valley shear zone, Nevada, *Geology*, *20*, 1107–1110.

Ebinger, C. J. (1989a), Tectonic development of the western branch of the East African Rift System, *Bull. Geol. Soc. Am.*, *101*, 885–903.

Ebinger, C. J. (1989b), Geometric and kinematic development of border faults and accommodation zones, Kivu-Rusizi Rift, Africa, *Tectonics*, *8*, 117–133.

Ebinger, C. J., A. L. Deino, R. E. Drake, and A. L. Tesha (1989), Chronology of volcanism and rift basin propagation: Rungwe Volcanic Province, East Africa, *J. Geophys. Res.*, *94*, 15,785–15,803.

Faccenna, C., R. Funiciello, A. Bruni, M. Mattei, and L. Sagnotti (1994a), Evolution of a transfer related basin: The Ardea basin (Latium, central Italy), *Basin Res.*, *6*, 35–46.

Faccenna, C., R. Funiciello, and M. Mattei (1994b), Late Pleistocene N-S shear zones along the Latium Tyrrhenian margin: Structural characters and volcanological implications, *Boll. Geofis. Teor. Appl.*, *36*, 507–522.

Faccenna, C., T. Nalpas, J. P. Brun, P. Davy, and V. Bosi (1995), The influence of pre-existing thrust faults on normal fault geometry in nature and in experiments, *J. Struct. Geol.*, *17*, 1139–1149.

Faccenna, C., M. Mattei, R. Funiciello, and L. Jolivet (1997), Styles of back-arc extension in the central Mediterranean, *Terra Nova*, *9*, 126–130.

Faccenna, C., F. Funiciello, D. Giardini, and P. Lucente (2001), Episodic Back-arc extension during restricted mantle convection in the central Mediterranean, *Earth Planet. Sci. Lett.*, *187*, 105–116.

Faulds, J. E., and R. J. Varga (1998), The role of accommodation zones and transfer zones in the regional segmentation of extended terranes, *Spec. Pap. Geol. Soc. Am.*, *323*, 1–45.

Fazzini, P., and R. Gelmini (1982), Tettonica trasversale nell'appennino settentrionale, *Boll. Soc. Geol. Ital.*, *24*, 299–309.

Fedi, M., and A. Rapolla (1987), The Campanian volcanic area: Analysis of magnetic and gravimetric anomalies, *Boll. Soc. Geol. Ital.*, *196*, 793–805.

Ferrari, L., S. Conticelli, L. Burlamacchi, and P. Manetti (1996), Volcanological evolution of the Monte Amiata, southern Tuscany: New geological and petrochemical data, *Acta Vulcanol.*, *8*, 41–56.

Ferrill, D. A., J. A. Stamatakos, and D. Sims (1999), Normal fault corrugation: Implications for growth and seismicity of active normal faults, *J. Struct. Geol.*, *21*, 1027–1038.

Finetti, I., and C. Morelli (1974), Esplorazione sismica a riflessione dei Golfi di Napoli e Pozzuoli, *Boll. Geofis. Teorica Appl.*, *16*, 175–222.

Funiciello, R., E. Locardi, and M. Parotto (1976), Lineamenti geologici dell'area Sabatina orientale, *Boll. Soc. Geol. Ital.*, *95*, 831–849.

Funiciello, F., C. Faccenna, D. Giardini, and K. Regenauer-Lieb (2003), Dynamics of retreating slabs: 2. Insights from three-dimensional laboratory experiments, *J. Geophys. Res.*, *108*(B4), 2207, doi:10.1029/2001JB000896.

Gamberi, F., and M. P. Marani (2004), Structural framework of the Tyrrhenian Sea unveiled by seafloor morphology, *Mem. Descr. Carta Geol. Ital.*, *XLIV*, 97–108.

Ghisetti, F., and L. Vezzani (1997), Interfering paths of deformation and development of arcs in the fold-and-thrust belt of the central Apennines (Italy), *Tectonics*, *16*, 523–536.

Ghisetti, F., and L. Vezzani (1999), Depth and modes of Pliocene-Pleistocene crustal extension of the Apennines (Italy), *Terra Nova*, *11*, 67–72.

Ghisetti, F., and L. Vezzani (2002), Normal faulting, transcrustal permeability and seismogenesis in the Apennines (Italy), *Tectonophysics*, *348*, 155–168.

Gianelli, G., A. Manzella, and M. Puxeddu (1997), Crustal models of the geothermal areas of southern Tuscany (Italy), *Tectonophysics*, *281*, 221–239.

Gibbs, A. D. (1984), Structural evolution of extensional basin margins, *J. Geol. Soc. London*, *141*, 609–620.

Gibbs, A. D. (1990), Linked faults in basin formation, *J. Struct. Geol.*, *12*, 795–803.

Giordano, G., G. Naso, D. Scrocca, R. Funiciello, and F. Catalani (1995), Processi di estensione e circolazione di fluidi a bassa termalità nella piana di Riardo (Caserta, Appennino centro-meridionale), *Boll. Soc. Geol. Ital.*, *114*, 361–371.

Hutchinson, D. R., A. J. Golmshtok, L. P. Zonenshain, T. C. Moore, C. A. Scholz, and K. D. Klitgord (1992), Depositional and tectonic framework of the rift basins of Lake Baikal from multichannel seismic data, *Geology*, *20*, 589–592.

Illies, J. H. (1975), Recent and paleo-intraplate tectonics in stable Europe and the Rhine graben Rift System, *Tectonophysics*, *29*, 251–264.

Jolivet, L., et al. (1998), Midcrustal shear zones in post-orogenic extension: Example from the northern Tyrrhenian Sea, *J. Geophys. Res.*, *103*, 12,123–12,160.

Krantz, R. W. (1989), Orthorombic fault patterns: The odd axis model and slip vector orientations, *Tectonics*, *8*, 483–495.

La Torre, P., R. Nannini, and F. Sollevanti (1981), Geothermal exploration in central Italy: Geophysical surveys in Cimini Range area, paper presented at European Association of Exploration Geophysicists Meeting, Venice, Italy.

Liotta, D. (1991), The Arbia-Val Marecchia Line, northern Apennines, *Eclogae Geol. Helv.*, *84*(2), 413–430.

Locardi, E., and R. Nicolich (1988), Geodinamica del Tirreno e dell'Appennino centro-meridionale: La nuova carta della Moho, *Mem. Soc. Geol. Ital.*, *41*, 121–140.

Locardi, E., G. Lombardi, R. Funiciello, and M. Parotto (1976), The main volcanic groups of Latium (Italy): Relations between structural evolution and petrogenesis, *Geol. Romana*, 279–300.

Mack, G. H., and W. R. Seager (1995), Transfer zones in the southern Rio Grande Rift, *J. Geol. Soc. London*, *152*, 551–560.

Malinverno, A., and W. B. F. Ryan (1986), Extension in the Tyrrhenian Sea and shortening in the Apennines as result of arc migration driven by sinking of the lithosphere, *Tectonics*, *5*, 227–245.

Mariani, M., and R. Prato (1988), I bacini neogenici costieri del margine tirrenico: Approccio sismico-stratigrafico, *Mem. Soc. Geol. Ital.*, *41*, 519–531.

Marra, F. (2001), Strike-slip faulting and block rotation: A possible triggering mechanism for lava flows in the Alban Hills?, *J. Struct. Geol.*, *23*, 127–141.

Martin, M. W., A. F. Glazner, J. D. Walker, and E. R. Schermer (1993), Evidence for right lateral transfer faulting accommodating en echelon Miocene extension, Mojave Desert, California, *Geology*, *21*, 355–358.

Marzocchi, W., R. Scandone, and F. Mulargia (1993), The tectonic setting of Mount Vesuvius and the correlation between its eruptions and the earthquakes of the southern Apennines, *J. Volcanol. Geotherm. Res.*, *58*, 27–41.

Mattei, M., R. Funiciello, and C. Kissel (1995), Paleomagnetic and structural evidence for Neogene block rotations in the central Apennines, Italy, *J. Geophys. Res.*, *100*, 17,863–17,883.

Mattei, M., P. Cipollari, D. Casentino, A. Argentieri, F. Rossetti, F. Speranza, and L. Di Bella (2002), The Miocene tectono-sedimentary evolution of the southern Tyrrhenian Sea: Stratigraphy, structural and paleomagnetic data from the on-shore Amantea basin (Calabrian arc, Italy), *Basin Res.*, *14*, 147–168.

Matteini, M., R. Mazzuoli, R. Omarini, R. Cas, and R. Maas (2002), The geochemical variations of the upper Cenozoic volcanism along the Calama-Olacapato-El Toro transversal fault system in central Andes (~24°S): Petrogenetic and geodynamic implications, *Tectonophysics*, *345*, 211–227.

McClay, K., and S. Khalil (1998), Extensional hard linkages, eastern Gulf of Suez, Egypt, *Geology*, *26*, 563–566.

Mele, G., and E. Sandvol (2003), Deep crustal roots beneath the northern Apennines inferred from teleseismic receiver functions, *Earth Planet. Sci. Lett.*, *211*, 69–78.

Milani, E. J., and I. Davison (1988), Basement control and transfer tectonics in the Reconcavo-Tucano-Jatoba rift, northeast Brazil, *Tectonophysics*, *154*, 41–70.

Monaco, C., and L. Tortorici (2000), Active faulting in the Calabrian arc and eastern Sicily, *J. Geodyn.*, *29*, 407–424.

Monaco, C., P. Tapponier, L. Tortorici, and P. Y. Gillot (1997), Late Quaternary slip rates on the Acireale-Piedimonte normal faults and tectonic origin of Mt. Etna (Sicily), *Earth Planet. Sci. Lett.*, *147*, 125–139.

Montone, P., A. Amato, and S. Pondrelli (1999), Active stress map of Italy, *J. Geophys. Res.*, *104*, 25,595–25,610.

Morewood, N. C., and G. P. Roberts (2000), The geometry, kinematics and rates of deformation within an en-echelon normal fault segment boundary, central Italy, *J. Struct. Geol.*, *22*, 1027–1047.

Morley, C. K. (1988), Variable extension in Lake Tanganyika, *Tectonics*, *7*, 785–801.

Morley, C. K., R. A. Nelson, T. L. Patton, and S. G. Munn (1990), Transfer zones in the East African Rift System and their relevance to hydrocarbon exploration in rifts, *AAPG Bull.*, *74*, 1234–1253.

Nappi, G., A. Renzulli, and P. Santi (1987), An evolutionary model for the Paleo-Bolsena and Bolsena Volcanic complexes: A structural and petrographic study, *Period. Mineral.*, *56*, 241–267.

Nappi, G., A. Renzulli, and P. Santi (1991), Evidence of incremental growth in the Vulsinian calderas (central Italy), *J. Volcanol. Geotherm. Res.*, *47*, 13–31.

Nelson, R. A., T. L. Patton, and C. K. Morley (1992), Rift-segment interaction and its relation to hydrocarbon exploration in continental rift systems, *AAPG Bull.*, *76*, 1153–1169.

Nicolich, R. (1989), Crustal structures from seismic studies in the frame of the European geotraverse (southern segment) and CROP project, in *The Lithosphere in Italy*, edited by A. Boriani et al., pp. 41–61, Accad. Naz. Lincei, Rome.

Norini, G., G. Groppelli, A. M. F. Lagmay, and L. Capra (2005), The Tenango Fault: Active intra-arc transtensive deformation in the central Trans-Mexican Volcanic Belt, paper presented at the 2005 European Geophysical Union Assembly, Vienna, Austria.

Oldow, J. S., B. D'Argenio, L. Ferranti, G. Pappone, E. Marsella, and M. Sacchi (1993), Large-scale longitudinal extension in the southern Apennines contractional belt, Italy, *Geology*, *21*, 1123–1127.

Orlando, L., M. Bernabini, G. Bertini, G. M. Cameli, and I. Dini (1991), Interpretazione preliminare del minimo gravimetrico del M. Amiata, *Studi Geol. Camerti.*, *1994*(1), 175–181.

Orsi, G., S. De Vita, and M. di Vito (1996), The restless, resurgent Campi Flegrei nested caldera (Italy): Constrains on its evolution and configuration, *J. Volcanol. Geotherm. Res.*, *74*, 179–214.

Patacca, E., R. Sartori, and P. Scandone (1990), Tyrrhenian basin and apenninic arcs: Kinematic relations since late Tortonian times, *Mem. Soc. Geol. Ital.*, *45*, 425–451.

Peccerillo, A., S. Conticelli, and P. Manetti (1987), Petrological characteristics and the genesis of the recent magmatism of southern Tuscany and northern Latium, *Period. Mineral.*, *56*, 157–172.

Piochi, M., P. P. Bruno, and G. De Astis (2005), Relative roles of rifting tectonics and magma ascent processes: Inferences from geophysical, structural volcanological and geochemical data for the Neapolitan volcanic region (southern Italy), *Geochem. Geophys. Geosyst.*, *6*, Q07005, doi:10.1029/2004GC000885.

Poli, S., S. Chiesa, P. Y. Gillot, A. Gregnanin, and F. Guichard (1987), Chemistry versus time in the volcanic complex of Ischia (Gulf of Naples, Italy): Evidence of successive magmatic cycles, *Contrib. Mineral. Petrol.*, *95*, 322–335.

Ranalli, G. (1995), *Rheology of the Earth*, CRC Press, Boca Raton, Fla.

Rapolla, A., M. Fedi, and G. Fiume (1989), Crustal structure of the Ischia-Phlegraean geothermal fields, near Naples, Italy, from gravity and aeromagnetic data, *Geophys. J.*, *97*, 409–419.

Reches, Z. (1978), Analysis of faulting in three-dimensional strain field, *Tectonophysics*, *47*, 109–129.

Riller, U., I. A. Petrinovic, J. Ramelow, M. Strecker, and O. Oncken (2001), Late Cenozoic tectonism, collapse caldera and plateau formation in the central Andes, *Earth Planet. Sci. Lett.*, *188*, 299–311.

Roberts, G. P., and A. M. Michetti (2004), Spatial and temporal variations in growth rates along active normal fault systems: An example from the Lazio-Abruzzi Apennines, central Italy, *J. Struct. Geol.*, *26*, 339–376.

Rosendahl, B. R. (1987), Architecture of continental rifts with special reference to East Africa, *Annu. Rev. Earth Planet. Sci.*, *15*, 445–503.

Rosi, M., and A. Sbrana (1987), Phlegraean fields, *Quad. Ric. Sci.*, *114*, 167 pp.

Royden, L., E. Patacca, and P. Scandone (1987), Segmentation and configuration of subducted lithosphere in Italy: An important control on thrust-belt and foredeep-basin evolution, *Geology*, *15*, 714–717.

Ruppel, C. (1995), Extensional processes in continental lithosphere, *J. Geophys. Res.*, *100*, 24,187–24,125.

Sani, F., C. Del Ventisette, D. Montanari, M. Coli, P. Nafissi, and A. Piazzini (2004), Tectonic evolution of the internal sector of the central Apennines, Italy, *Mar. Pet. Geol.*, *21*, 1235–1254.

Santacroce, R. (1987), *Somma Vesuvius*, 251 pp., Cons. Naz. delle Ric., Rome.

Scandone, R., F. Bellucci, L. Lirer, and G. Rolandi (1991), The structure of the Campanian Plain and the activity of the Neapolitan volcanoes (Italy), *J. Volcanol. Geotherm. Res.*, *48*, 1–31.

Schlische, R. W. (1992), Structural and stratigraphic development of the Newark extensional basin, eastern North America: Evidence for the growth of the basin and its bounding structures, *Geol. Soc. Am. Bull.*, *104*, 1246–1263.

Serri, G. F., F. Innocenti, and P. Manetti (1993), Geochemical and petrological evidence of the subduction of delaminated Adriatic continental lithosphere in the genesis of the Neogene-Quaternary magmatism of central Italy, *Tectonophysics*, *223*, 117–147.

Sherman, S. I. (1978), Faults of the Baikal rift zone, *Tectonophysics*, *45*, 31–39.

Spadini, G., and Y. Podladchikov (1996), Spacing of consecutive normal faulting in the lithosphere: A dynamic model for rift axis jumping (Tyrrhenian Sea), *Earth Planet. Sci. Lett.*, *144*, 21–34.

Spakman, W., and M. J. R. Wortel (2005), A tomographic view on western Mediterranean geodynamics, paper presented at the 2005 European Geophysical Union Assembly, Vienna, Austria.

Spinks, K., V. Acocella, J. Cole, and K. Bassett (2005), Structural control of volcanism and caldera development in the transtensional Taupo Volcanic Zone, New Zealand, *J. Volcanol. Geotherm. Res.*, *144*, 7–22.

Tibaldi, A. (1992), The role of transcurrent intra-arc tectonics in the configuration of a volcanic arc, *Terra Nova*, *4*, 567–577.

Tsikalas, F., J. I. Faleide, and O. Eldholm (2001), Lateral variations in tectono-magmatic style along the Lofoten-Vesteralen volcanic margin off Norway, *Mar. Pet. Geol.*, *18*, 807–832.

Turco, E., and A. Zuppetta (1998), A kinematic model for the Plio-Quaternary evolution of the Tyrrhenian-Apenninic system: Implications for rifting processes and volcanism, *J. Volcanol. Geotherm. Res.*, *82*, 1–18.

Turcotte, D. L., and G. Schubert (1982), *Geodynamics: Application of Continuum Physics to Geological Problems*, 450 pp., John Wiley, Hoboken, N. J.

Turi, B., H. P. Taylor, and G. Ferrara (1991), Comparisons of $^{18}O/^{16}O$ and $^{87}Sr/^{86}Sr$ in volcanic rocks from the Pontine Islands, M. Ernici and Campania with other areas in Italy, *Spec. Publ. Geochem. Soc.*, *3*, 307–324.

Valensise, G., and D. Pantosti (2001), Database of potential sources for earthquakes larger than M 5.5 in Italy, *Ann. Geofis.*, *44*, 797–964.

van Bergen, M. J., and M. Barton (1984), Complex interaction of aluminous metasedimentary xenoliths and siliceous magma: An example from Mt. Amiata (central Italy), *Contrib. Mineral. Petrol.*, *86*, 374–385.

Vezzoli, L. (1988), *Island of Ischia*, 135 pp., Cons. Naz. delle Ric., Rome.

Vezzoli, L., S. Conticelli, F. Innocenti, P. Landi, P. Manetti, D. M. Palladino, and R. Trigila (1987), Stratigraphy of the Latera Volcanic complex: Proposals for a new nomenclature, *Period. Mineral.*, *56*, 89–110.

Vigneresse, J. L. (1995), Crustal regime of deformation and ascent of granitic magma, *Tectonophysics*, *249*, 187–202.

Watterson, J., J. Walsh, A. Nicol, P. A. R. Nell, and P. G. Bretan (2000), Geometry and origin of a polygonal fault system, *J. Geol. Soc. London*, *157*, 151–162.

Watts, A. B., and J. Stewart (1998), Gravity anomalies and segmentation of the continental margin offshore West Africa, *Earth Planet. Sci. Lett.*, *156*, 239–252.

Ziegler, P. A., and S. Cloething (2004), Dynamic processes controlling the evolution of rifted basins, *Earth Sci. Rev.*, *64*, 1–50.

V. Acocella and R. Funiciello, Dipartimento Scienze Geologiche, Università Roma Tre, Largo S. L. Murialdo, 1, I-00146 Rome, Italy. (acocella@uniroma3.it)